Auto-inhibition of adenylyl cyclase 9 (AC9) by an isoform-specific motif in the carboxyl-terminal region

Graphical Abstract

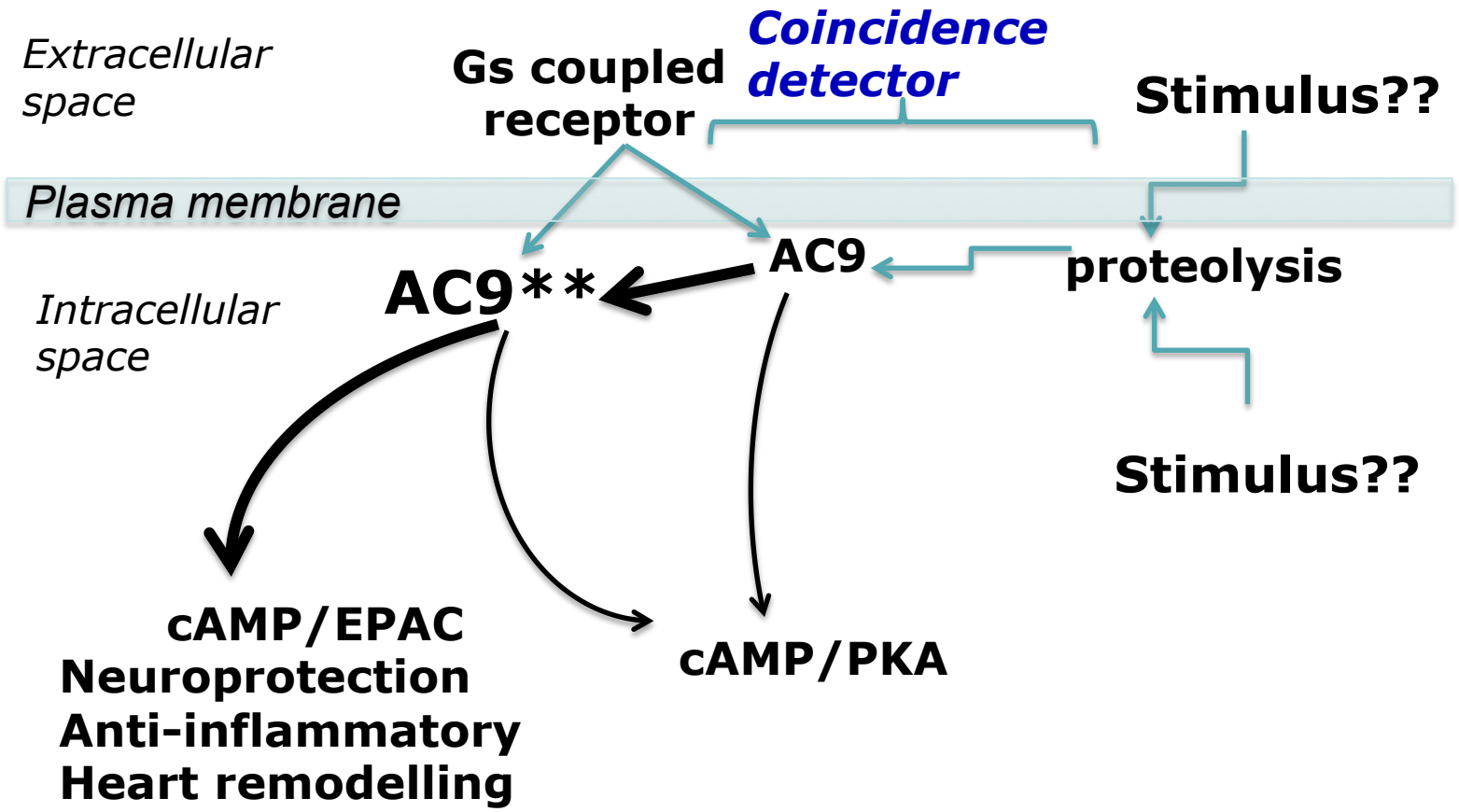

Highlights

- AC9 is a trans-membrane adenylyl cyclase highly expressed in the brain and the heart.
- The response of AC9 to the activation of Gs-coupled receptors (GsCR) is low.
- A stretch of nine AA-residues in the COOH-tail of AC9 blunts the response to GsCR.
- COOH-terminally cleaved AC9 was detected in rodent and human heart.
- Proteases may gate the activation of AC9 by cleaving the auto-inhibitory COOH-tail.

Auto-inhibition of adenylyl cyclase 9 (AC9) by an isoform-specific motif in the carboxyl-terminal region.

Adrienn Pálvölgyi[1], James Simpson[2], Ibolya Bodnár[1], Judit Bíró[1], Miklós Palkovits[3], Tamás Radovits[4], Paul Skehel[2], Ferenc A. Antoni[1,2]

[1] Division of Preclinical Research, Egis Pharmaceuticals PLC, Budapest, Hungary

[2] Centre for Discovery Brain Sciences, Deanery of Biomedical Sciences University of Edinburgh, Edinburgh, Scotland, U.K.,

[3] Human Brain Tissue Bank and Laboratory, Semmelweis University, Budapest,

[4] Semmelweis University Heart and Vascular Center, Budapest, Hungary,

Corresponding author: Ferenc A. Antoni

Centre for Discovery Brain Sciences, University of Edinburgh,

Edinburgh EH8 9XD, Scotland, U.K.

Phone: +44 796 864 7338

mailto:ferenc.antoni@ed.ac.uk

mailto:franzantoni@gmail.com

ABSTRACT

Trans-membrane adenylyl cyclase (tmAC) isoforms show markedly distinct regulatory properties that have not been fully explored. AC9 is highly expressed in vital organs such as the heart and the brain. Here, we report that the isoform-specific carboxyl-terminal domain (C2b) of AC9 inhibits the activation of the enzyme by Gs-coupled receptors (GsCR). In human embryonic kidney cells (HEK293) stably overexpressing AC9, cAMP production by AC9 induced upon the activation of endogenous β-adrenergic and prostanoid GsCRs was barely discernible. Cells expressing AC9 lacking the C2b domain showed a markedly enhanced cAMP response to GsCR. Subsequent studies of the response of AC9 mutants to the activation of GsCR revealed that residues 1268-1276 in the C2b domain were critical for auto-inhibition. Two main species of AC9 of 130K and ≥170K apparent molecular weight were observed on immunoblots of rodent and human myocardial membranes with NH_2-terminally directed anti-AC9 antibodies. The lower molecular weight AC9 band did not react with antibodies directed against the C2b domain. It was the predominant species of AC9 in rodent heart tissue and some of the human samples. There is a single gene for AC9 in vertebrates, moreover, amino acids 957-1353 of the COOH-terminus are encoded by a single exon with no apparent signs of mRNA splicing or editing making it highly unlikely that COOH-terminally truncated AC9 could arise through the processing or editing of mRNA. Thus, deductive reasoning leads to the suggestion that proteolytic cleavage of the C2b auto-inhibitory domain may govern the activation of AC9 by GsCR.

Key words: auto-inhibition; adenylyl cyclase, cyclic AMP, myocardium; limited proteolysis; heart failure.

1. INTRODUCTION

Trans-membrane adenylyl cyclases (tmAC) are integral membrane proteins that produce the ubiquitous intracellular messenger adenosine 3'5' monophosphate (cAMP) from ATP. Similar to other intracellular signalling proteins, tmAC are produced from a family of genes giving rise to nine isoforms of tmAC with distinct regulatory properties [1-3]. However, knowledge about the exact function and biological significance of the isoform specific regulation in tmAC is far from complete [3, 4]. The schematic structure of tmAC is shown in Fig.1A. The catalytic core of the enzyme is formed through non-covalent interactions between the C1a and C2a cytoplasmic domains [5]. The primary amino acid sequence of these domains is relatively well-conserved between paralogues of tmAC. In contrast, the NH_2-terminal domain, the trans-membrane domains, as well as the cytoplasmic C1b and C2b domains show low sequence homology between the isoforms [2, 3]. In turn, the isoform-specific sequences show minimal interspecies variation in vertebrates, indicating that the isoform-specific facets of tmAC function are governed by these parts of the protein. The present study analysed the contribution of the C2b domain to the regulatory properties of trans-membrane adenylyl cyclase 9 (AC9) [6]. First, this focus was prompted by the wide variation in the size of the C2b domain – in AC2 it consists of about 11 amino acid residues whereas in AC9 it is 111. Second, a considerable number of studies have been reported with a human AC9 clone (dfm_AC9), [3, 7, 8] that has a double frame-shift mutation close to the start of the C2b domain (Fig 1 A and C). As a result, the C2B domain of dfm_AC9 is shorter, and of different primary sequence than that of AC9 (Fig 1C). Thus, it was of interest to compare the properties of what appears to be the physiological version of the enzyme with those of this mutant. While basal cAMP production by AC9 could be readily analysed in HEK293 cells stably expressing mouse [9] or human AC9 [10] the activation of the enzyme by GsCR in these cells was poor. A similar observation has

been published by Rhee et al [11] using COS 7 cells as the *in transfecto* context. We now report the identification of a short motif in the C2b domain of AC9 occupying positions 1268-1276 in the protein chain, that suppresses the activation of the enzyme by receptor-activated Gs. Moreover, we provide evidence that AC9 is subject to limited COOH-terminal proteolysis in the heart indicating that auto-inhibition by the C2b domain is a relevant mechanism of biological control.

2. MATERIALS AND METHODS

2.1 Site-directed mutagenesis

The human AC9 cDNA previously reported [10] was subcloned into pcDNA3.1 (Invitrogen). Mutations were introduced by site-directed mutagenesis with custom-designed primers using Phusion High-Fidelity DNA Polymerase (Thermo Fisher Scientific Waltham, MA USA) as per the manufacturer's instructions. The resulting constructs were verified by DNA sequencing of the entire coding region (Biomi Ltd, Gödöllő, Hungary). COOH-terminally truncated AC9 versions are indexed by the single letter code of last amino acid and its position before the stop codon. For example, AC9_Y1242 is the version truncated at the junction of the C2a and C2b domains. The primary sequence of the COOH-terminal from position 1240 is shown in Fig 1B.

2.2 Cell culture

Stable human embryonic kidney cell (HEK 293) lines obtained upon transfection using Metafectene Pro (Biontex Laboratories GmbH) with cDNAs encoding human AC9, AC9 ending at residue Y1242 (AC9_1242) or the skeleton vector pcDNA3.1

were maintained under antibiotic selection using neomycin (0.6 mg/ml), in Dulbecco's MEM supplemented with 10 v/v% fetal bovine serum. These cells were pated on 96-well culture plates (Greiner Hungary Ltd, Mosonmagyaróvár, Hungary) at a density of 5 x 10^4 cells/ well and used 48h later to analyse the cAMP response to isoproterenol and PGE_2.

A HEK293 cell line stably expressing 5-HT_{7A} receptors (^{3}H-SB269970 binding capacity for crude membrane protein: 20±3 pmol/mg protein, mean ±S.E.M. n=4) was also produced and maintained under neomycin selection. These cells were transiently transfected by the calcium-phosphate method [12] with the expression vectors of the requisite wild-type and variously mutated AC9 cDNAs. Forty-eight h after transfection, the cells were detached from the culture dishes with Ca^{2+}-, Mg^{2+}-free HBSS (Sigma H 6648) supplemented with 3 mM Na_2EDTA (pH 8), pelleted by cenrifugation at 800 x g for 10min, resuspended and replated at a density of 10^5 cells/well in flat-bottom 96-well plates coated with poly-L-lysine (Sigma SIAL0596). The cells were used 24 h later to analyse the cAMP response to 5-HT. The rest of the cells (5 x 10^6 /transfection), was plated on 150 mm diameter round tissue culture plates and collected at 72h after transfection for ligand binding assay and the subsequent analysis of AC9 expression by immunoblots. In some experiments, COS7 cells were subjected to the same transfection regime, except that a pcDNA3.1 based expression plasmid for the human 5-HT_{7A} receptor was co-transfected with AC9. At least two independent transfections were carried out for each AC9 mutant tested in this study.

2.3 Assay of cAMP production

The culture medium was removed, and HAM's F10 medium was added (100 µl/well, Gibco, 31550-031). The cells were incubated for 2.5 h at 37°C in a tissue culture incubator in an atmosphere of 95%O_2-5% CO_2. Subsequently, the cells were washed once with warm HBSS supplemented with 10 mM HEPES, pH 7.4 and incubated in 100µl of the same medium at 37°C. After 20 min, 50 µl fresh medium was added supplemented with 2 mM isobutylmethylxanthine (Sigma, I5879) and the cells were incubated at 37°C in a total volume of 150 µl. Fifteen minutes later, 50 µl of agonist solution were added and the incubation was continued at 37°C, for various time intervals. The incubation was terminated by the addition of 50 µl of ice-cold 0.5 M HCl. In agonist concentration-response studies the incubation of the wells was uniformly terminated at 15 min as by that time the cAMP concentration of the cells plus medium reached a steady-state plateau. In some cases, the assay was carried out under Ca^{2+}-depleting conditions [9, 13], with no added Ca^{2+}, 1mM EGTA and 1 µM ionomycin (Sigma, I9657) introduced at the addition HBSS. Upon the termination of the incubation, the concentration of cAMP in the wells was quantified by radioimmunoassay [13].

2.4 Ligand-binding assay for 5-HT_{7A} receptors

Frozen pellets of HEK293 cells stably expressing 5-HT_{7A} receptors were resuspended in homogenization buffer (50 mM HEPES buffer with 27% Sucrose, 5 mM EDTA, pH 7.5) and rapidly refrozen for 30 min at -80 °C. After thawing, the cells were homogenized for 30 sec at setting 7 with a T-25 IKA Ultraturrax homogenizer and centrifuged for 5 min at 300 x g, 4°C. The supernatant was centrifuged 20 min at 27,000 x g, 4 °C. The pellet was resuspended in 50 mM HEPES buffer supplemented 1 mM EDTA, pH 7.5. Centrifugation and resuspension were repeated once more. The crude membranes were diluted in the binding reaction buffer (50 mM Tris-HCl, 10 mM $MgSO_4$, 0,5 mM EDTA, pH 7.5) and incubated with ^{3}H-SB-269970 (New

England Nuclear) for 120 min at room temperature. The bound and the free tracer fractions were separated by filtration over Whatman GF/C filters presoaked in 0.3% (w/v) polyethyleneimine. After copious washing with buffer (50 mM Tris-HCl, 10 mM $MgSO_4$, 0,5 mM EDTA, pH 7.5) the filters were dried and the amount of radioactivity attached to the filters was quantified by liquid scintillation counting in a Perkin-Elmer Top-Count NXT or Packard Tri-Carb 2900TR instrument. Ligand-binding curves were fitted by non-linear regression using Graphpad Prism v. 6.0 and K_d and B_{max} values were calculated with the "one site – specific binding" equation.

2.5 Immunocytochemistry

HEK293 cells stably expressing WT human AC9 and AC9_Y1242 were plated on poly-D-lysine-coated coverslips and cultured as described above. Two to four days after plating, the coverslips were briefly washed with phosphate-buffered saline (PBS) and exposed to Zamboni's fixative, pH 7.4, for 20 min at 4°C. Following fixation the cells were processed for immunostaining as previously reported [10]. Primary antibodies: affinity-purified rabbit antibodies (1:1000) raised against the NH_2-terminal region and affinity purified sheep antibodies (1:1000) against the COOH-terminus of human AC9 [9]. Secondary antibodies: Alexa fluor 488-conjugated donkey anti-rabbit IgG (Invitrogen A21206) and Alexa fluor 594-conjugated donkey anti-sheep IgG (Invitrogen A-11016) were applied at 1:500 for 1 hr at RT. After several washes in PBS, the specimens were mounted in CitiFluor (Sigma) and viewed under a Bio-Rad Radiance 2100 Rainbow confocal microscope.

2.6 Animals

Male NMRI mice bred in house were used at 20–30 g BW, adult male C57/BL6J mice of similar BW weight range were from Taconic labs. All animals were housed under standard laboratory conditions (24 ± 2 ºC, 40–60% relative humidity), on a 12 h light/dark cycle with light onset at 6:00 AM. The left ventricle of the heart from adult

NMRI or C57/BL6 mice was obtained after rapid decapitation/exsanguination. The excised tissues were briefly rinsed in ice-cold PBS, frozen on dry ice and stored at -80°C prior to further processing.

2.7 Immunoblots

For the analysis of the cells examined for cAMP production, batches of transfected cells were processed for immunoblotting. Cells were detached from the culture plates in ice-cold HBSS (Sigma H 6648) supplemented with 1 mM EDTA, centrifuged at 1000 x g for 1 min at 4°C. The resulting cell-pellet was homogenized by trituration with a 1ml Gilson Microman pipette tip in homogenization buffer (0.5M $NaCO_3$, pH11, containing 1 mM EDTA, 1 mM EGTA and 15µl/ml of protease inhibitor cocktail (Sigma, P8340). This buffer enriches the membranes for integral membrane proteins by stripping non-integral interacting proteins [14-16]. The homogenate was centrifuged at 1000xg for 10 min at 4°C and the resultant supernatant was further centrifuged at 100,000 x g for 40 min in a Beckman mini ultracentrifuge at 4°C (Beckman Coulter Optima Max-XP). The pellet was re-suspended in 50mM sodium phosphate buffer pH 7.2, containing 2% SDS (w/v), 5% 2-mercaptoethanol (v/v) and adjusted to 1mg/ml protein or lower depending on the anticipated AC9 concentration of the sample. SDS-PAGE and blotting onto Immobilon-FL, PVDF membranes (Merck-Millipore) were carried out in a Phast-Gel apparatus as previously reported [9]. Blots were blocked by LiCor blocking solution at RT for 60 min, washed with PBS-0.1% Tween-20 and incubated overnight at 4°C with primary antibodies. These were i) affinity purified rabbit antibodies directed against the NH_2-terminal region common in mouse and human AC9 [9], ii) affinity-purified rabbit or sheep antibodies directed against the final fifteen COOH-terminal amino acid residues of human AC9 [9], iii) a rabbit antiserum directed against the C2b paralogue-specific domain of mouse AC9 [17] kindly supplied by Dr. Richard Premont – also see Fig. 1A. In some cases, the rabbit anti-NH_2-terminal and the sheep anti-COOH terminus antibodies

were applied in combination. In blots from transient transfection studies, a mouse monoclonal antibody against N+K+-ATPAse (Millipore 05-369 | Anti-Na+/K+ ATPase α-1 Antibody, clone C464.6) was used at 1:2000 dilution as a housekeeping marker for the amount of plasma membranes present. Following the exposure to primary antibodies, the blots were washed with PBS-0.1% Tween-20 for 5 x 5 min and reacted with the requisite secondary reagents, selected from: IRDye 680LT Conjugated Goat (polyclonal) Anti-Rabbit IgG (H+L) (LI-COR, 926-68021), IRDye 800CW Conjugated Goat (polyclonal) Anti-Mouse IgG (H+L) (LI-COR, 926-32210), IRDye® 680LT Donkey anti-Goat IgG (H + L), 0.1 mg (925-68024), IRDye® 800CW Donkey anti-Goat IgG (H + L), 0.1 mg (925-32214) and incubated under constant rotation at RT for 60 min. Blots were washed with PBS-0.1% Tween-20, air-dried, and subsequently imaged with a LiCor Odyssey dual laser imager, using the LICOR ImageStudio 2.1.12. software. Immunoreactive band intensities were calculated after local background substraction and are given as arbitrary units. The ratio of the intensities of the AC9 immunoreactive band over the Na^+K^+ATP-ase immunoreactive band for each group of transfected cells was calculated and used to standardize the levels of cAMP production in that group.

Well-characterized human myocardial tissue samples from the anterior wall of the left ventricle were obtained from the Transplantation Biobank of the Heart and Vascular Center at Semmelweis University, Budapest, Hungary. Following institutional and national ethical committee approval and informed consent from organ donor family members or end-stage heart failure patients undergoing heart transplantation, myocardial tissue samples were surgically removed, immediately frozen in liquid nitrogen, and stored at -80°C. Human brain samples from the hippocampus and the anterior cingulate cortex were collected and stored frozen by M. Palkovits at the Human Brain Tissue Bank of the Semmelweis University, Budapest, Hungary.

Mouse and human tissue samples were homogenized from frozen in ice-cold carbonate based homogenization buffer with a Ultra-Turrax T-25 homogenizer by two 1 min bursts at setting 7, and crude membranes for SDS-PAGE were prepared as described above for HEK293 cells .

2.8 Data analysis

In transient transfection studies, the amount of cAMP per well was divided by the amount of protein in the well. Agonist-evoked standardized cAMP was calculated as follows: the respective baseline cAMP levels measured in the presence of IBMX were substracted from the values obtained in the presence of agonist. The corresponding values from the group expressing the pcDNA3.1 skeleton vector were substracted to eliminate the contribution of the endogenous cAMP production of the host cells. In the case of wild type AC9, this sometimes resulted in negative values at low concentrations of agonist. The values of net cAMP production thus obtained were corrected for the level of AC9 protein expression by multiplying with the ratio of the intensities of the AC9 and Na+K+-ATPase immunoreactive bands relevant for the batch of transfection. In the case of COS-7 cells where the human 5-HT_{7A} receptor was contransfected with the AC9 variants, the binding capacity for ^{3}H-SB-269970 was also taken into account — cAMP production was divided by the ^{3}H-SB-269970 binding capacity of the membranes. Data are reported as individual data points or mean±S.D. Each experimental condition was tested in at least two independent studies. Data analysis was carried out with GraphPad Prism v6. As the standard deviation of the cAMP data was proportional to the respective means the data were analysed after log transformation. Results from stably transfected cells and time course studies of transiently transfected cells were analysed by two-way ANOVA followed by Tukey's test for multiple comparisons. Dose response curves for 5-HT in transient transfections were assayed in duplicate except for the basal (n=4) and the highest concentration of 5-HT (1µM) applied (n=3). In these cases the cAMP

response to 1µM 5-HT was analysed as an index of the maximal response by Student's t-test or one-way ANOVA followed by Dunnett's *post-hoc* test as appropriate.

2.9 Ethical declaration: All animal experimental protocols were approved by the Animal Care and Use Ethical Committee of Egis Pharmaceuticals PLC and complied with the Hungarian Law of Animal Care and Use (1998. XVIII). The Human Tissue Bank, Semmelweis University, Hungary is a member of the Brain Net II Europe consortium. All procedures performed in studies involving human participants were in accordance with the ethical standards of the institutional and national research committee and with the 1964 Declaration of Helsinki and its later amendments. Ethical permission numbers: 6008/8/2002/ETT and 32/1992/TUKEB for HBTB; ETT TUKEB 7891/2012/EKU (119/PI/12.) and TUKEB 73/2005 for myocardial samples.

3. RESULTS

3.1 Auto-inhibition of AC9 by a short motif in the C2b domain

Basal cAMP accumulation in HEK293 cells stably transfected with AC9 or AC9_Y1242 was studied in the presence of 0.5 mM IBMX. As shown in Fig. 2A, both cell lines containing AC9 had much higher unstimulated cAMP levels than cells expressing the pcDNA3.1 skeleton vector. HEK293 cells express endogenous $ß_2$-adrenergic receptors [18]. Accordingly, isoproterenol produced a robust increase of cAMP levels in the presence of 0.5 mM IBMX in cells stably transfected with the skeleton vector pcDNA3.1 (Fig 2B). However, cells stably expressing high levels of human AC9 [10] showed only marginal enhancement of the cAMP response to isoproterenol when compared with the response of the host cells containing pcDNA3.1. Removal of the isoform-specific C2b domain resulted in an isoproterenol-

induced cAMP response that was several-fold greater than that observed in pcDNA3.1 cells (Fig. 2B). Similar data were obtained with PGE_2 as the agonist (Fig. 2C). Immunostaining with NH_2- and COOH-terminal directed antibodies showed no major differences in the cellular localization or the level of expression of wild type AC9 and AC9_Y1242 (Fig. 3) in HEK 293 cells. Cell expressing the skeleton vector pcDNA3.1 showed no AC9 immunopositive reaction (Supplementary Fig 2). Immunoblots (Fig. 3B) showed the expected full-length AC9 immunoreactive band at around 170 K [9, 10], a minor band reactive with the COOH-terminal antibody was also detected at around 90 K. Anti-NH_2-terminal antibody avidly detected AC9-Y1242 as a protein of lower molecular weight than AC9 that gave no reaction with the anti-COOH terminus antibody (Fig 3B). No immunopositive protein bands were found in pcDNA3.1 containing cells (Supplementary Fig 3).

In order to exclude modifications of cAMP metabolism arising from the long-term overexpression of AC9, the requisite AC9 expression plasmids were transiently transfected into HEK293 stably expressing 5-HT_{7A} receptors. Transient transfection with AC9 or AC9_Y1242 had no significant effect on the levels of 5-HT_{7A} receptors as determined by [^{3}H]-SB269970 binding (data not shown). Importantly, the marked enhancement of the agonist-evoked cAMP response upon removal of the C2b domain was also evident in this system (Fig. 4A). The effect of cell context on the apparent auto-inhibitory role of the C2b domain was tested in COS-7 cells co-transfected with $5HT_{7A}$ receptor cDNA and the requisite AC9 cDNAs. As shown in Fig. 4B, the pattern of the cAMP response to 5-HT in COS-7 cells was closely similar to that seen in HEK293 cells. Finally, these studies also showed that truncation at V1288 does not alter the response of AC9 to GsCR activation (Fig. 4A & B).

In order to delineate the segment of the C2b domain required for auto-inhibition of the agonist-induced activation of AC9, further COOH-terminally truncated mutants (see Fig. 1B) of AC9 were tested. When compared with AC9 and AC9_Y1242, the

COOH-terminally truncated versions showed binary, all-or-none characteristics with respect to cAMP formation induced by 5-HT. Specifically, while AC9_D1276 yielded a cyclase that had a low cAMP response to 5-HT identical to that of full-length AC9 (Fig. 5A&C), AC9_D1268 produced a cAMP response closely similar to that of AC9_Y1242 (Fig. 5B&D). The raw cAMP data of these studies are shown in Supplementary fig 5 and 6). We also compared the stimulation of AC9 with that of dfm_AC9, as the C2b domain of the latter has a completely different sequence at positions 1268-1276 (Fig. 1C). As shown in Fig. 6, the standardized cAMP response of dfm_AC9 to 5-HT was several-fold greater than that of AC9, resembling the properties of AC9_Y1242.

Finally, we tested the effects of mutations placed in the purported autoinhibitory domain (residues 1268-1276) of full-length AC9 (Fig. 7A). Mutation of the SPTD motif to AAAA produced a cyclase that was stimulated by 5-HT to a greater degree than AC9, but not reaching the cAMP response of AC9_Y1242 (Fig. 7B). As S1273 is a potential phosphorylation site of prolyl-directed protein kinases, the mutation S1273A was also tested. The effect was to significantly enhance the cAMP response to 5-HT, although to a much smaller extent than that seen with AC9_C2a (Fig. 6B).

Taken together, our *in transfecto* experiments showed that the paralogue-specific C2b domain of AC9 exerts a marked auto-inhibitory effect on the activation of the enzyme by a variety of GsCRs. We have previously reported a COOH-terminally truncated species of AC9 in rat brain and AtT20 pituitary tumour cells [9, 10, 19]. As the COOH-terminus of AC9 is encoded by a single large exon from residues 957 to 1353, and no signs of mRNA splicing or editing are apparent, we examined heart and brain tissue for signs of proteolytic alterations of AC9.

3.2 Two main forms of AC9 in rodent and human heart

Interestingly, the main species of AC9 expressed in the left ventricle of mouse heart appeared COOH-terminally truncated as it failed to react with the COOH-terminally directed antibodies (Fig. 9 A & B) and was of lower molecular weight (≈130K) than the full-length AC9 observed in HEK293 cells (Fig 2 B). Full-length AC9 in mouse heart was barely detectable by an antibody raised against the entire C2b domain [17] that readily reacted with AC9_1267 transfected into HEK293 cells, but failed to detect AC9_Y1242, confirming its specificity towards the C2b domain (Fig 8D). This observation strongly suggests that the auto-inhibitory segment consisting of residues 1268-1276 is missing from the 130K AC9 species in mouse heart. A more complex picture emerged when membranes from a healthy control and five failing human hearts obtained from heart transplant donor and recipient patients, respectively, were examined for AC9 immunoreactive bands (Fig. 9). Importantly, in three of the samples (Tx22, Tx24, Tx32), a distinct immunoreactive band migrating at ≈130K was detected by NH_2-terminal but not COOH-terminal anti-AC9 (Fig. 9A&B). This band co-migrated with the NH_2-reactive AC9 band from mouse hearts (Fig. 9C). In one of these samples, (Tx24) a COOH-terminally reactive AC9 band was only barely detectable with any of the three antibodies (sheep or rabbit anti-COOH-terminal AC9, both affinity purified, rabbit anti-C2b). In order to exclude post-homogenization artefacts, two independent samples were processed from each heart with identical results.

In adult post-mortem human hippocampus and anterior cingulate cortex a ≈160 K species of AC9, that consistently migrated below the ≈170 K band from heart, predominated. This band was COOH-terminally intact, as indicated by the reaction with the extreme COOH-terminal directed antibodies (Fig 9D). The less intense lower mass bands obtained with the NH_2-terminal antibody were not investigated further.

4. DISCUSSION

The present study shows that the C2b isoform-specific domain of AC9 exerts a marked auto-inhibitory effect on the activation of the enzyme by GsCR. Moreover, in the absence of data supporting alternative splicing of AC9 mRNA encoding the COOH-terminal region AC9, the results from mouse, as well as human heart suggest, that proteolytic cleavage of the C2b domain may gate the activation of AC9 in the heart by relieving the autoinhibitory effect.

4.1 Auto-inhibition of AC9 in transfecto

In transfecto, the stimulation of AC9 by endogenous receptors in HEK 293 cells was barely discernible. In contrast, robust activation occurred upon reducing the length of the C2b domain to residue D1267 or by Ala mutations of residues within the 1268-1277 sequence. Our analysis was restricted to studies in intact cells, thus the mechanistic underpinnings of the C2b effect and the kinetic parameters of auto-inhibition remain to be explored. The whole cell approach is justified, as the auto-inhibitory effect may not be faithfully translatable in a cell-free system e.g. see ref [20]. Moreover, the use of a PDE blocker likely distorted the quantitative relationships, but was technically unavoidable. Nevertheless, it is clear from the data presented that, through residues 1268 to 1276, the isoform-specific C2b domain exerts a major inhibitory effect on the activation of AC9 by GsCR. Interestingly, the auto-inhibitory motif is in a segment of the C2b domain that is phylogenetically highly conserved in vertebrates (Supplementary Fig. 8). Within this motif, S1273 was shown to contribute to the auto-inhibitory effect. As S1273 is potentially phosphorylated by prolyl-directed kinases that are highly active in HEK293 cells [6, 21] it may well represent a cell context-specific element of the auto-inhibitory effect.

.

Auto-inhibition is a potentially important issue for the physiological control of tmAC. As the mature enzyme courses through the endoplasmic reticulum network, the cytoplasmic loops are in the correct orientation for activation, provided Mg^{2+}ATP is present. It is currently hypothesized that the C1a-C2a complex is stable *in vivo* and stimulation of enzyme activity by $G_{s\alpha}$-GTP or the diterpene drug forskolin is by optimization of the catalytically active conformation of the heterodimer [22]. Alternatively, it is possible that the C1a-C2a complex is not abundant *in vivo* and its formation is enhanced by $G_{s\alpha}$ or forskolin [23]. Taken together, the findings imply that one of the roles of the isoform-specific domains could be to prevent physiologically irrelevant activation of tmACs. Indeed, previous, largely biochemical studies in cell free systems have implicated the C1b [24] and the NH_2-terminal [25] domains in the inhibitory control of AC6, and the C1b domain in the inhibition of AC7 [26]. Our studies are the first to show auto-inhibitory control of a tmAC by C2b, which is operational in intact cells.

Soluble AC (sAC) has also been reported to contain an auto-inhibitory domain close to the COOH-terminal end of the C2 catalytic domain, reviewed in [27]. The primary sequence required for auto-inhibition of AC9 has no obvious resemblance to that identified in sAC [27]. Furthermore, the biological relevance of the auto-inhibition in sAC is unknown.

A side-product of our analysis is that it clearly differentiates a major functional characteristic of the dfm-AC9 clone [7] from that of full-length AC9: the former lacks the C2b auto-inhibitory sequence and consequently generates a dramatically enhanced cAMP response to GsCR activation when compared with AC9. There is a single gene for AC9 in both the mouse and the human genomes. Moreover, the exon_intron architecture of the mouse as well as the human AC9 genes is similar, in

that residues 957-1353 (i.e. from the end of the TM2 domain through to the COOH-terminus) to are encoded by a single, large exon. There are no apparent alternative mRNA splicing sites in this segment of the either the mouse or the human gene. In agreement, the mRNA analysis of mouse heart AC9 by RT-PCR failed to show evidence for mRNA splicing or editing (See Supplement section 1). Thus, the biological relevance of dfm-AC9, originally cloned from a commercial human cardiac cDNA library [7], requires further study.

4.2 Limited proteolysis and AC9

Auto-inhibition relieved by limited proteolysis is a well-known regulatory mechanism in proteins [28]. Activation of tmACs by proteolysis has been described in several earlier studies [29-32]. However, no clear biological relevance could be provided for these observations and none of them seems to have been followed up in the longer term.

A COOH-terminally truncated ≈130 K form of AC9 appeared to be the predominant species of the enzyme in membranes prepared from rodent left ventricular heart tissue. It is likely, that the bulk of the enzyme is in the myocardium [33]. A similar AC9 form, that gave no reaction with antibodies directed against the COOH-terminus, was previously detected in AtT20 mouse pituitary tumour cells [9, 19]. The lack of a reaction of the 130 K AC9 species with the anti-C2b serum that readily detected recombinantly expressed AC9_D1268 and AC9_D1276 indicates that the auto-inhibitory domain is not present in this form of the enzyme. This is consonant with a previous report of rat heart with the same antiserum [17]. However, at present, it cannot be fully ruled out, that the anti-C2b serum is not sensitive enough to detect physiological levels of AC9 with only a small part of the C2b domain present. Full length, ≈170K, COOH-terminally intact AC9 could be also detected at low levels in mouse heart. Similar, ≈130 K and ≈170 K AC9 NH_2-terminal immunoreactive bands

were present in the six human samples tested. In three of the samples (Tx22, 24 and 32), the 130 K species appeared substantially more abundant than the 170 K one. However, at present no correlation with the clinical data is apparent that would explain this finding (T. Radovits personal communication).

As to which protease(s) may be involved in the cleavage of AC9 is currently a matter of speculation. Previously, we reported that AC9 was readily cleaved in hippocampal membranes by a Ca^{2+}-dependent protease activity that was blocked by selective inhibitors of calpain [34]. Interestingly, no such activity could be discerned in HEK 293 cells [34]. Further work is required to clarify the site(s) of cleavage in the enzyme and the proteases involved.

4.3 Functional implications

A plausible consequence of increased cAMP generation by COOH-terminally cleaved AC9 is the amplitude modulation, i.e. a quantitative aspect, of the cAMP response. Whilst protein kinase A is fully stimulated at 1µM cAMP, other effector systems modulated by cAMP such as exchange protein directly activated by cAMP (EPAC) and hyperpolarization-activated cyclic nucleotide-gated (HCN) channels require greater than 10µM cAMP to be active, reviewed in refs. [3, 4, 35]. HCN channels are relevant as pacemaker channels regulating the frequency of action potentials in the heart [36] as well as the CNS [37]. EPACs are involved in cardiac remodelling processes [35, 38] in which Ca^{2+}-activated proteases such calpains and/or caspases are thought to play a prominent role [39, 40]. Could proteolytic disinhibition of AC9 be the link between caspase/calpain activation and EPAC signalling leading to remodelling of the heart? In a yet further cardiac context, AC9 in myocardiocytes associates with the A-kinase anchoring protein *yotiao*, which also complexes KCNQ1 potassium ion channel subunits important for heart repolarization reviewed in ref. [33]. Genetic deletion of AC9 is mostly embryonic lethal [6, 41, 42],

but a small fraction of AC9 null homozygotes survive [42, 43]. Examination of the cardiac function of these animals [43] showed that the cAMP-dependent phosphorylation of the heat-shock protein *Hsp20* is compromised, raising the possibility that AC9 in the heart may have a cardioprotective role [44]. Taken together, switching of the responsiveness of AC9 *via* proteolysis in the C2b domain may determine the spectrum of intracellular cAMP effectors activated in a complex extracellular stimulus environment such as that seen in neuronal development or myocardial hypertrophy.

In conclusion, the data presented here demonstrate a potent auto-inhibitory motif in the isoform-specific COOH-terminal C2b domain of AC9. Moreover, the existence of a COOH-terminally truncated species of AC9 in the heart raises the possibility that the auto-inhibitory effect is relieved by limited proteolysis. Further work is warranted to examine the latter issue.

5. ACKNOWLEDGEMENTS

5.1 Funding

This work was supported by the Medical Research Council, U.K. , the Servier-Egis Research Co-operation Agreement, project no. NVKP_16-1-2016-0017 ('National Heart Program') funded by the National Research, Development and Innovation Fund of Hungary.

5.2 External input

We thank Dr Richard T. Premont (Duke University, Durham, NC, USA, for the generous provision of anti-C2b domain AC9 antiserum, the Dept. of Anatomy, Histology and Embryology at Semmelweis University, Budapest for access to their confocal microscope facility, Professor Béla Merkely (Semmelweis University Heart and Vascular Center, Budapest) for his support of the project, and Professor Péter

Enyedi, (Semmelweis University, Dept. of Physiology) for critical discussions and the provision of laboratory facilities.

6. DISCLOSURES

6.1 Conflict of interest

AP, IB, JB, FAA were employees of Egis Pharmaceuticals PLC, Budapest, Hungary.

6.2 Contributions:

AP, JS, IB, JB carried out experiments, collated and analyzed data, MP, TR provided unique samples collected by them and contributed to the manuscript, PS carried out experiments, analyzed data and contributed to the manuscript, FAA designed experiments, analyzed and collated data, wrote the manuscript. All authors have agreed on the text of the submitted manuscript.

7. REFERENCES

[1] R. Taussig, A.G. Gilman, Mammalian membrane-bound adenylyl cyclases, J. Biol. Chem. 270 (1995) 1-4.

[2] F.A. Antoni, Molecular diversity of cyclic AMP signaling, Front. Neuroendocrinol. 21 (2000) 103-132.

[3] C.W. Dessauer, V.J. Watts, R.S. Ostrom, M. Conti, S. Dove, R. Seifert, International Union of Basic and Clinical Pharmacology. CI. Structures and small molecule modulators of mammalian adenylyl cyclases, Pharmacol. Rev. 69 (2017) 93-139.

[4] F.A. Antoni, New paradigms in cAMP signalling, Mol. Cell. Endocrinol. 353 (2012) 3-9.

[5] J. Tesmer, S. Sprang, The structure, catalytic mechanism and regulation of adenylyl cyclase, Curr. Opin. Struct. Biol. 8 (1998) 713-9.

[6] F.A. Antoni, ADCY9 (Adenylyl cyclase 9), in: S. Choi (Ed.), Encyclopedia of Signaling Molecules, Springer International Publishing, Cham, 2018, pp. 170-175.

[7] B.M. Hacker, J.E. Tomlinson, G.A. Wayman, R. Sultana, G. Chna, E. Villacres, C. Disteche, D.R. Storm, Cloning, chromosomal mapping, and regulatory properties of the human type 9 adenylyl cyclase (ADCY9), Genomics 50 (1998) 97-104.

[8] M.G. Cumbay, V.J. Watts, Novel regulatory properties of human type 9 adenylate cyclase, J. Pharmacol. Exp. Ther. 310 (2004) 108-115.

[9] F.A. Antoni, M. Palkovits, J. Simpson, S.M. Smith, A.L. Leitch, R. Rosie, G. Fink, J.M. Paterson, Ca2+/calcineurin-inhibited adenylyl cyclase, highly abundant in forebrain regions important for learning and memory, J. Neurosci. 18 (1998) 9650-61.

[10] J.M. Paterson, S.M. Smith, J. Simpson, O.C. Grace, A.A. Sosunov, J.E. Bell, F.A. Antoni, Characterisation of human adenylyl cyclase IX reveals inhibition by Ca(2+)/Calcineurin and differential mRNA polyadenylation, J. Neurochem. 75 (2000) 1358-67.

[11] M.H. Rhee, M. Bayewitch, T. Avidor-Reiss, R. Levy, Z. Vogel, Cannabinoid receptor activation differentially regulates the various adenylyl cyclase isozymes, J. Neurochem. 71 (1998) 1525-34.

[12] P. Salmon, D. Trono, Production and titration of lentiviral vectors, Curr. Protoc. Neurosci. Chapter 4 (2006) Unit 4 21.

[13] F.A. Antoni, R.J. Barnard, M.J. Shipston, S.M. Smith, J. Simpson, J.M. Paterson, Calcineurin feedback inhibition of agonist-evoked cAMP formation, J. Biol. Chem. 270 (1995) 28055-61.

[14] K.S. Song, S. Li, T. Okamoto, L.A. Quilliam, M. Sargiacomo, M.P. Lisanti, Co-purification and direct interaction of Ras with caveolin, an integral membrane protein of caveolae microdomains. Detergent-free purification of caveolae microdomains, J. Biol. Chem. 271 (1996) 9690-7.

[15] C. Huang, J.R. Hepler, L.T. Chen, A.G. Gilman, R.G. Anderson, S.M. Mumby, Organization of G proteins and adenylyl cyclase at the plasma membrane, Mol. Biol. Cell 8 (1997) 2365-78.

[16] C. Schwencke, M. Yamamoto, S. Okumura, Y. Toya, S.J. Kim, Y. Ishikawa, Compartmentation of cyclic adenosine 3',5'-monophosphate signaling in caveolae, Mol. Endocrinol. 13 (1999) 1061-70.

[17] R.T. Premont, I. Matsuoka, M.G. Mattei, Y. Pouille, N. Defer, J. Hanoune, Identification and characterization of a widely expressed form of adenylyl cyclase, J. Biol. Chem. 271 (1996) 13900-7.

[18] E.M. Rosethorne, R.J. Turner, R.A. Fairhurst, S.J. Charlton, Efficacy is a contributing factor to the clinical onset of bronchodilation of inhaled β_2-

adrenoceptor agonists, Naunyn Schmiedeberg's Arch. Pharmacol. 382 (2010) 255-263.

[19] F.A. Antoni, U.K. Wiegand, J. Black, J. Simpson, Cellular localisation of adenylyl cyclase: a post-genome perspective, Neurochem. Res. 31 (2006) 287-95.

[20] G. Zimmermann, R. Taussig, Protein kinase C alters the responsiveness of adenylyl cyclases to G protein alpha and betagamma subunits, J. Biol. Chem. 271 (1996) 27161-6.

[21] D.P. Mohapatra, J.S. Trimmer, The Kv2.1 C terminus can autonomously transfer Kv2.1-like phosphorylation-dependent localization, voltage-dependent gating, and muscarinic modulation to diverse Kv channels, J. Neurosci. 26 (2006) 685-95.

[22] J.J. Tesmer, R.K. Sunahara, R.A. Johnson, G. Gosselin, A.G. Gilman, S.R. Sprang, Two-metal-Ion catalysis in adenylyl cyclase, Science 285 (1999) 756-60.

[23] R.E. Whisnant, A.G. Gilman, C.W. Dessauer, Interaction of the 2 cytosolic domains of mammalian adenylyl-cyclase, Proc. Natl. Acad. Sci. U. S. A. 93 (1996) 6621-6625.

[24] Y. Chen, A. Harry, J. Li, M.J. Smit, X. Bai, R. Magnusson, J.P. Pieroni, G. Weng, R. Iyengar, Adenylyl cyclase 6 is selectively regulated by protein kinase A phosphorylation in a region involved in Galphas stimulation, Proc. Natl. Acad. Sci. U. S. A. 94 (1997) 14100-4.

[25] H.L. Lai, T.H. Lin, Y.Y. Kao, W.J. Lin, M.J. Hwang, Y. Chern, The N terminus domain of type VI adenylyl cyclase mediates its inhibition by protein kinase C, Mol. Pharmacol. 56 (1999) 644-50.

[26] S.Z. Yan, J.A. Beeler, Y. Chen, R.K. Shelton, W.J. Tang, The regulation of type 7 adenylyl cyclase by its C1b region and Escherichia coli peptidylprolyl isomerase, SlyD, J. Biol. Chem. 276 (2001) 8500-6.

[27] C. Steegborn, Structure, mechanism, and regulation of soluble adenylyl cyclases - similarities and differences to transmembrane adenylyl cyclases, Biochim. Biophys. Acta 1842 (2014) 2535-47.

[28] M.A. Pufall, B.J. Graves, Autoinhibitory domains: modular effectors of cellular regulation, Annu. Rev. Cell. Dev. Biol. 18 (2002) 421-62.

[29] N.D. Richert, R.J. Ryan, Proteolytic enzyme activation of rat ovarian adenylate cyclase, Proc. Natl. Acad. Sci. U. S. A. 74 (1977) 4857-61.

[30] D. Stengel, P.M. Lad, T.B. Nielsen, M. Rodbell, J. Hanoune, Proteolysis activates adenylate cyclase in rat liver and AC-lymphoma cell independently of the guanine nucleotide regulatory site, FEBS Lett. 115 (1980) 260-4.

[31] J. Tremblay, P. Hamet, Calcium-dependent proteolytic stimulation of adenylate cyclase in platelets from spontaneously hypertensive rats, Metabolism 33 (1984) 689-95.

[32] T. Ebina, Y. Toya, N. Oka, J. Kawabe, C. Schwencke, Y. Ishikawa, Isoform-dependent activation of adenylyl cyclase by proteolysis, FEBS Lett. 401 (1997) 223-226.

[33] T.A. Baldwin, C.W. Dessauer, Function of adenylyl cyclase in heart: The AKAP connection, J. Cardiovasc. Dev. Dis. 5 (2018) doi:10.3390/jcdd5010002.

[34] F.A. Antoni, J. Simpson, Calcium-dependent proteolysis of adenylyl cyclase IX (ACIX), Biochem. Soc. Trans. 30 (3) A85 (2002).

[35] T. Fujita, M. Umemura, U. Yokoyama, S. Okumura, Y. Ishikawa, The role of Epac in the heart, Cell. Mol. Life Sci. 74 (2017) 591-606.

[36] P. Scicchitano, S. Carbonara, G. Ricci, C. Mandurino, M. Locorotondo, G. Bulzis, M. Gesualdo, A. Zito, R. Carbonara, I. Dentamaro, G. Riccioni, M.M. Ciccone, HCN channels and heart rate, Molecules 17 (2012) 4225-35.

[37] M. Biel, C. Wahl-Schott, S. Michalakis, X. Zong, Hyperpolarization-activated cation channels: from genes to function, Physiol. Rev. 89 (2009) 847-85.

[38] L. Pereira, G. Ruiz-Hurtado, E. Morel, A.-C. Laurent, M. Métrich, A. Domínguez-Rodríguez, S. Lauton-Santos, A. Lucas, J.-P. Benitah, D.M. Bers, F. Lezoualc'h, A.M. Gómez, Epac enhances excitation-transcription coupling in cardiac myocytes, J. Mol. Cell. Cardiol. 52 (2012) 283-291.

[39] A.S. Galvez, A. Diwan, A.M. Odley, H.S. Hahn, H. Osinska, J.G. Melendez, J. Robbins, R.A. Lynch, Y. Marreez, G.W. Dorn, 2nd, Cardiomyocyte degeneration with calpain deficiency reveals a critical role in protein homeostasis, Circ. Res. 100 (2007) 1071-8.

[40] E. Letavernier, L. Zafrani, J. Perez, B. Letavernier, J.P. Haymann, L. Baud, The role of calpains in myocardial remodelling and heart failure, Cardiovasc. Res. 96 (2012) 38-45.

[41] V. Perez-Garcia, E. Fineberg, R. Wilson, A. Murray, C.I. Mazzeo, C. Tudor, A. Sienerth, J.K. White, E. Tuck, E.J. Ryder, D. Gleeson, E. Siragher, H. Wardle-Jones, N. Staudt, N. Wali, J. Collins, S. Geyer, E.M. Busch-Nentwich, A. Galli, J.C. Smith, E. Robertson, D.J. Adams, W.J. Weninger, T. Mohun, M. Hemberger, Placentation defects are highly prevalent in embryonic lethal mouse mutants, Nature 555 (2018) 463.

[42] R. Wilson, S. Geyer, L. Reissig, e. al., Highly variable penetrance of abnormal phenotypes in embryonic lethal

knockout mice. , Wellcome Open Research 1:1 (doi: 10.12688/wellcomeopenres.9899.2) (2017).

[43] Y. Li, T.A. Baldwin, Y. Wang, J. Subramaniam, A.G. Carbajal, C.S. Brand, S.R. Cunha, C.W. Dessauer, Loss of type 9 adenylyl cyclase triggers reduced phosphorylation of Hsp20 and diastolic dysfunction, Sci. Rep. 7 (2017) 5522.

[44] H.V. Edwards, J.D. Scott, G.S. Baillie, PKA phosphorylation of the small heat-shock protein Hsp20 enhances its cardioprotective effects, Biochem. Soc. Trans. 40 (2012) 210-4.

8. LEGENDS TO THE FIGURES

Figure 1. Scheme of the protein/DNA sequences and antibodies relevant for this study **A)** The classic scheme of AC9 structure spanning the plasma membrane. The arrow indicates the site of the start of the isoform-specific C2B domain at Y1242. The scheme also shows the approximate sites of the epitopes of the primary antibodies used in this study. **B)** Single letter amino acid code of the C2b domain of human AC9, arrowheads highlight the COOH-terminal truncations tested in this study. **C)** Detail of the human AC9 cDNA sequence highlighting the double frame-shift mutation in the dfm_AC9 clone (Genebank accession no. AF036927) resulting in a change of the COOH-terminal sequence of the C2b domain from position P1252. The amino acid sequence of the mouse AC9 C2b domain (Genebank accession no. Z50190) is shown in the top row. Note the near identity with human AC9 AJ1333123.

Figure 2. Marked enhancement of stimulated cAMP formation upon deletion of the C2b domain of AC9 at residue Y1242. Studies in HEK293 cells stably transfected with skeleton vector (pcDNA3.1), human AC9 (AC9) or AC9 with the C2b domain removed at the cDNA level (AC9_Y1242). **A)** Time-course of cAMP accumulation upon the addition of 0.5 mM IBMX at time 0. Two-way ANOVA (10, 54) F=46.16, gave significant interaction. Tukey's post-hoc test showed that at all time points except 0 min, the levels of cAMP in the AC9 and AC9_Y1242 were significantly (P<0.001) higher than in the pcDNA3.1 group. At 30 and 40 min the levels of cAMP in AC9_Y1242 cells were significantly higher (*** P<0.001) than in cells AC9 containing AC9. **B)** Effect of the activation of endogenous β_2-adrenergic receptors by isoproterenol on cAMP production in the presence of 0.5 mM IBMX. Note marked enhancement of the cAMP response in AC9_Y1242 cells. 2-way

ANOVA gave significant interaction (8, 45) F=66 P<0.0001. Tukey's multiple comparisons test: **** P<0.0001 *vs.* pcDNA3.1, as well as AC9 groups, *P<0.05 *vs.* pcDNA3.1 **C)** Effect of the activation of endogenous of EP2-4 prostanoid receptors by PGE_2. Note marked enhancement of the cAMP response in AC9_Y1242 cells. 2-way ANOVA gave significant interaction (10, 54) F=105.5 P<0.0001. Tukey's multiple comparisons test: **** P<0.0001 *vs.* pcDNA3.1, as well as AC9 groups. Data are mean±S.D. n=4, and are representative of at least two independent experiments giving similar results.

Figure 3. Immunodetection for AC9 and AC9_Y1242 reveals no major differences in the distribution of the proteins in HEK293 cells. A) Stably transfected HEK293 cells were co-stained with affinity-purified primary rabbit (green) and sheep (red) antibodies directed against NH_2- and anti-COOH-terminal of human AC9, respectively. Note close proximity of the immunoreactivity to the plasma membrane and the absence of COOH-terminal staining cells expressing AC9_C2a. The bars represent 20 µm. **B)** Immunoblots of cell homogenates of HEK293 cells stably expressing human AC9 (lanes 1 and 2) or AC9_Y1242 (lanes 3 and 4). Blots were reacted with affinity-purified primary rabbit (red) and sheep (green) antibodies directed against the NH_2-terminal region and the COOH-terminus of human AC9, respectively.

Figure 4. The inhibitory effect of the C2b domain is independent of cell context. A) Effect of serotonin (5-HT) on cAMP accumulation in HEK293 cells stably expressing 5-HT_{7A} receptors and transiently transfected with AC9. Note the markedly enhanced response by AC9_Y1242 and that by AC9 truncated at residue V1288 (AC9_V1288) did not differ from that of wild-type AC9. Individual data points are shown. Inset: cAMP response at 1µM 5-HT, one-way ANOVA, F (2, 6) = 19.72, P = 0.0023, ** P<0.01 *vs.* AC9, Dunnett's test for multiple comparisons. Geometric

means, the bars represent S.D. **B)** Similar results were obtained in COS 7 cells co-transfected with 5-HT_{7A} receptors and the requisite AC9 variants. Individual data points are shown. Inset: cAMP response at 1µM 5-HT, one-way ANOVA F (2, 6) = 52.34, P = 0.0002, *** P<0.001 *vs.* AC9, Dunnett's test for multiple comparisons. Geometric means, the bars represent S.D. Data are representative of two independent experiments.

Figure 5. Comparison of the properties of AC9_D1276 and AC_D1267 shows an all-or-none type inhibitory effect of residues 1268-1277 (GSIGRSPTD). A) AC9_D1276**:** Time-course of cAMP production evoked by 15 nM 5-HT. Data are means ± S.D. n=3 /point. Two- way ANOVA gave significant interaction, F (12, 41) = 214.4, P < 0.0001, **** P<0.0001 *vs.* AC9 as well as AC9_D1276, Tukey's test for multiple comparisons. **B)** AC9_D1267: Time-course of cAMP production evoked by 15 nM 5-HT. Data are means ± S.D. n=3 /point. Two- way ANOVA gave significant interaction, F (12, 42)=23.16, P < 0.0001 , **** P<0.0001 *vs.* AC9. **C)** AC9_D1276: cAMP responses evoked by 5-HT, at 15 min after addition of the agonist. Individual data points are shown. Inset: cAMP response at 1µM 5-HT, one-way ANOVA, F (2, 6) = 84.29, P < 0.0001, , *** P<0.001 *vs.* AC9, Dunnett's test for multiple comparisons. Geometric means, the bars represent S.D. **D)** AC9_D1267: cAMP responses evoked by 5-HT, at 15 min after addition of the agonist. Individual data points are shown. Inset: cAMP response at 1µM 5-HT, one-way ANOVA, F (2, 6) = 422.1, P < 0.0001, **** P<0.0001 *vs.* AC9, Dunnett's test for multiple comparisons. Geometric means, the bars represent S.D. Data shown are representative of two independent experiments. Note all-or-none type effect of the deletion of residues 1268-1277 on the 5-HT-induced cAMP response.

Figure 6. The double frame-shift mutant human AC9 (dfm-AC9) has properties similar to AC9_Y1242. The 5-HT-evoked cAMP response attributable to dfm_AC9 is

comparable to that seen with AC9_Y1242. Individual data points are shown, representative of two independent experiments. Inset: cAMP response at 1μM 5-HT, *** P<0.001, Student's t-test. Data are representative of two independent experiments.

Figure 7. Mutations of the purported auto-inhibitory segment in full-length AC9 partially mimic the effects of COOH-terminal deletion. **A)** The site of the mutations within positions 1268-1277. **B)** The effects of the mutations on cAMP production evoked by 5-HT at 15 min after the addition of the agonist. Data are means ± S.D. n=3/point. Inset: cAMP response at 1μM 5-HT, one-way ANOVA, $F(3, 12) = 29.30$, $P < 0.0001$, * P<0.05, *** P<0.001, **** P<0.0001 *vs.* AC9, Dunnett's test for multiple comparisons. Geometric means, the bars represent S.D. Data are representative of at least two independent experiments.

Figure 8. A COOH-terminally truncated species of AC9 in mouse heart. Immunoblots of crude membranes prepared from the left ventricle of the heart of C57/Bl6 male mice were reacted with affinity-purified primary rabbit **(A)** and sheep **(B)** antibodies directed against the NH_2-terminal region and COOH-terminus of human AC9, respectively. Note faint COOH-terminal reactive band in mouse heart. **C)** The same samples analyzed with an antiserum raised against the entire C2b region of AC9 [17]. Note the lack of reaction with the relatively abundant ≈130K band detected by anti-NH_2-terminal antibodies. **D)** Partial characterization of the anti-C2b serum: immunoblots of crude membranes from HEK293 cells over-expressing AC9_D1267 (lane 1) AC9_D1276 (lane 2), full-length AC9 (lane 3) and AC9_Y1242 (lane 4). Note lack of reaction with AC9_Y1242, confirming the specificity of the antiserum for the C2b domain.

Figure 9. Presence of COOH-terminally truncated AC9 in human heart. A) Healthy control (HD) and failing (TX22-32) human hearts from transplant patients with different pathoaetiologies (TX22: myocarditis, TX23: restrictive cardiomyopathy, TX24: hypertrophic obstructive cardiomyopathy, TX31: ischemic heart disease, TX32: collagenosis) reacted with affinity-purified primary rabbit antibodies directed against the NH_2-terminal region of AC9. Note the presence of a ≈130 K AC9 species in all samples and the resolution of the ≈170 K band into a doublet in samples TX22 and Tx23. **B)** Immunoblots of the same samples reacted with affinity-purified primary rabbit antibodies directed against the COOH-terminus of human AC9. Note barely discernible ≈170 K band in sample Tx24. **C)** Samples from male mouse (C57/BL6, NMRI) and human hearts (Tx 23 and 24) reacted with affinity-purified primary rabbit antibodies directed against the NH_2-terminal region of AC9. Note close similarity in Rf for the ≈130 K AC9 species from mouse and human hearts. The full-length ≈170 K AC9 band was from HEK293 (AC9.1) cells stably transfected with human AC9. **D)** Immunoblot of human hippocampus (Hip) and anterior cingulate cortex (Cing) reacted with with affinity-purified primary rabbit antibodies directed against the NH_2-terminal region of AC9 (left panel) and affinity-purified sheep antibodies directed against the COOH-terminus of human AC9 (right panel).

Figure(s)

Fig. 1

A.

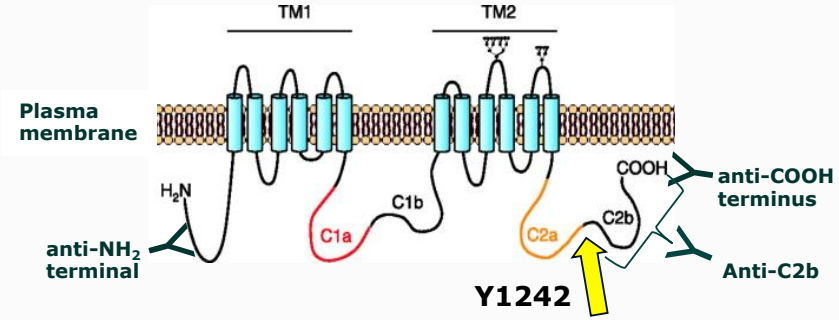

B. *Human AC9 C2b domain*

```
1240      1250      1260      1270      1280      1290    1300
|         |         |         |         |         |       |
YLYPKCTDHRVIPQHQLSISPDIRVQVDGSIGRSPTDEIANLVPSVQYVDKTSLGSDSSTQ
          1310      1320      1330      1340      1350
          |         |         |         |         |
AKDAHLSPKRPWKEPVKAEERGRFGKAIEKDDCDETGIEEANELTKLNVSKSV*
```

C.

```
Human AC9 AJ133123   (4277)   GATCAC AGGGTCATCC CACAGCACCA GCTGTCCATC TCCCCA
                     identity:  ...... .......... ..  ...... .......... ......
Human AC9 AF036927   (3755)   GATCAC AGGGTCATCC CA--GCACCA GCTGTCCATC TCCCCA
```

```
                1240      1250      1260      1270      1280      1290      1300
                |         |         |         |         |         |         |
Mouse           YLYPKCTDNGVVPQHQLSISPDIRVQVDGSIGRSPTDEIANLVPSVQYSDKASLGSDDSTQ...
AJ133123        YLYPKCTDHRVIPQHQLSISPDIRVQVDGSIGRSPTDEIANLVPSVQYVDKTSLGSDSSTQ...
AF036927        YLYPKCTDHRVIPAPAVHLPRHPRPGGWQHRTVSHRRDCQPGAFCPVCGQDISGF*
```

Figure 2.

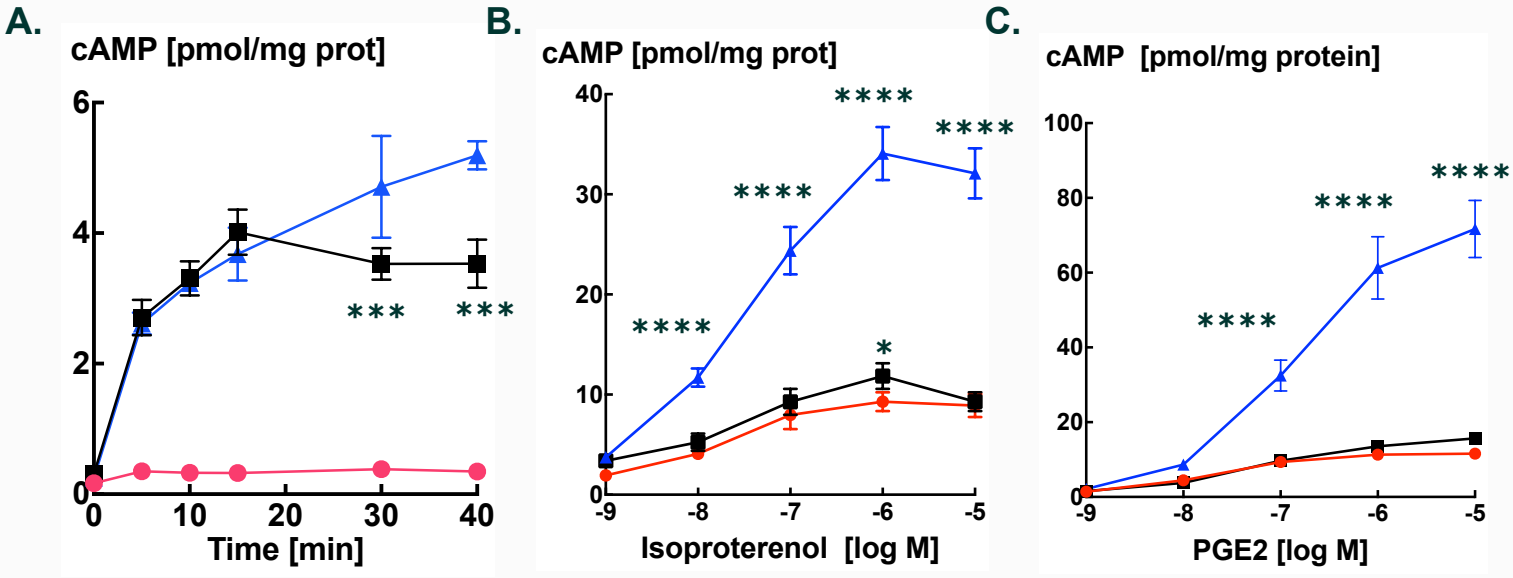
A.
cAMP [pmol/mg prot]
6
4
2
0
0
10
20
30
40
Time [min]
***
***
B.
cAMP [pmol/mg prot]
40
30
20
10
0
-9
-8
-7
-6
-5
Isoproterenol [log M]
****
****
****
****
*
C.
cAMP [pmol/mg protein]
100
80
60
40
20
0
-9
-8
-7
-6
-5
PGE2 [log M]
****
****
****

Fig. 3

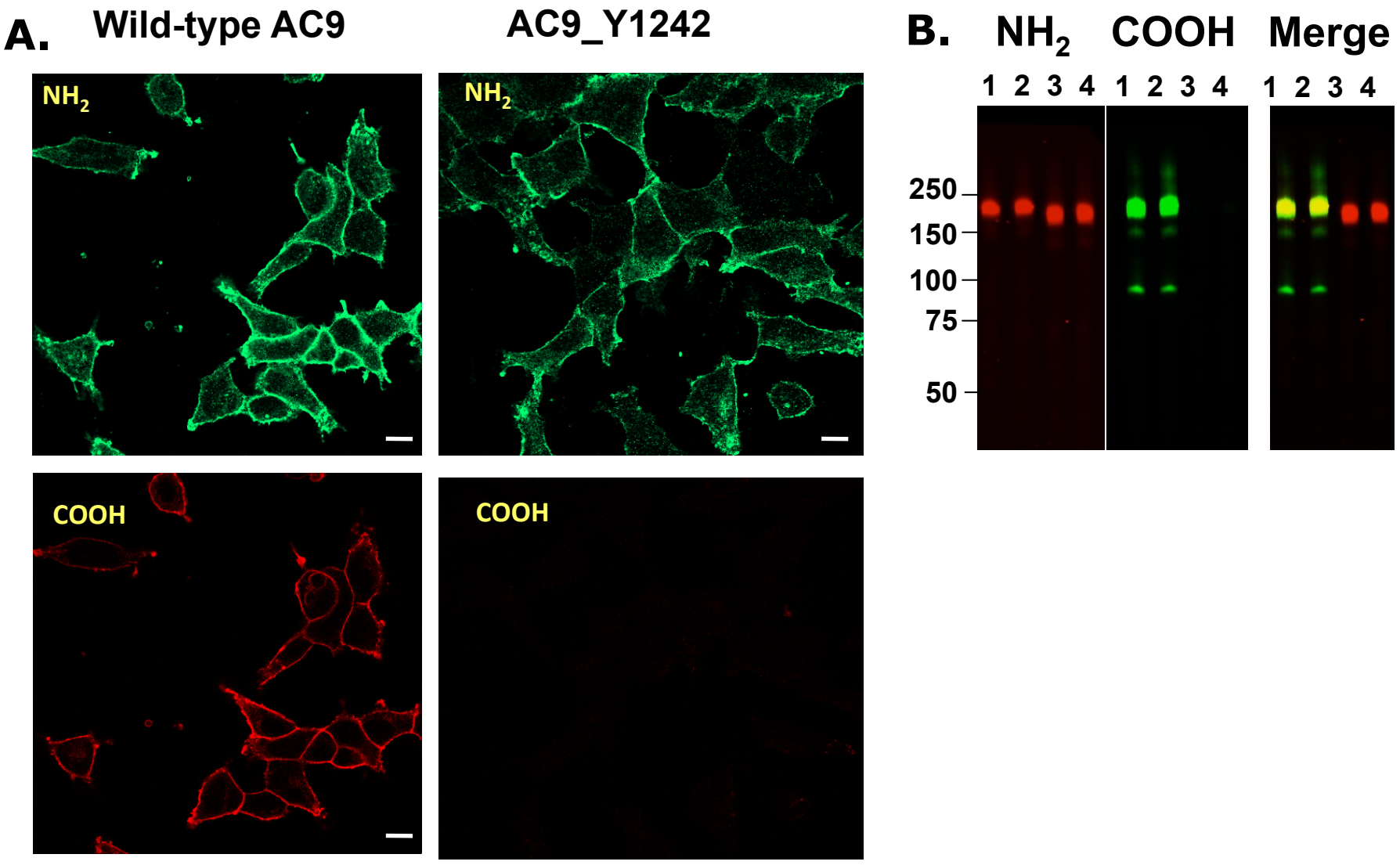
A.
Wild-type AC9
AC9_Y1242
NH2
NH2
COOH
COOH
B.
NH2
COOH
Merge
1 2 3 4 1 2 3 4 1 2 3 4
250
150
100
75
50

Fig. 4

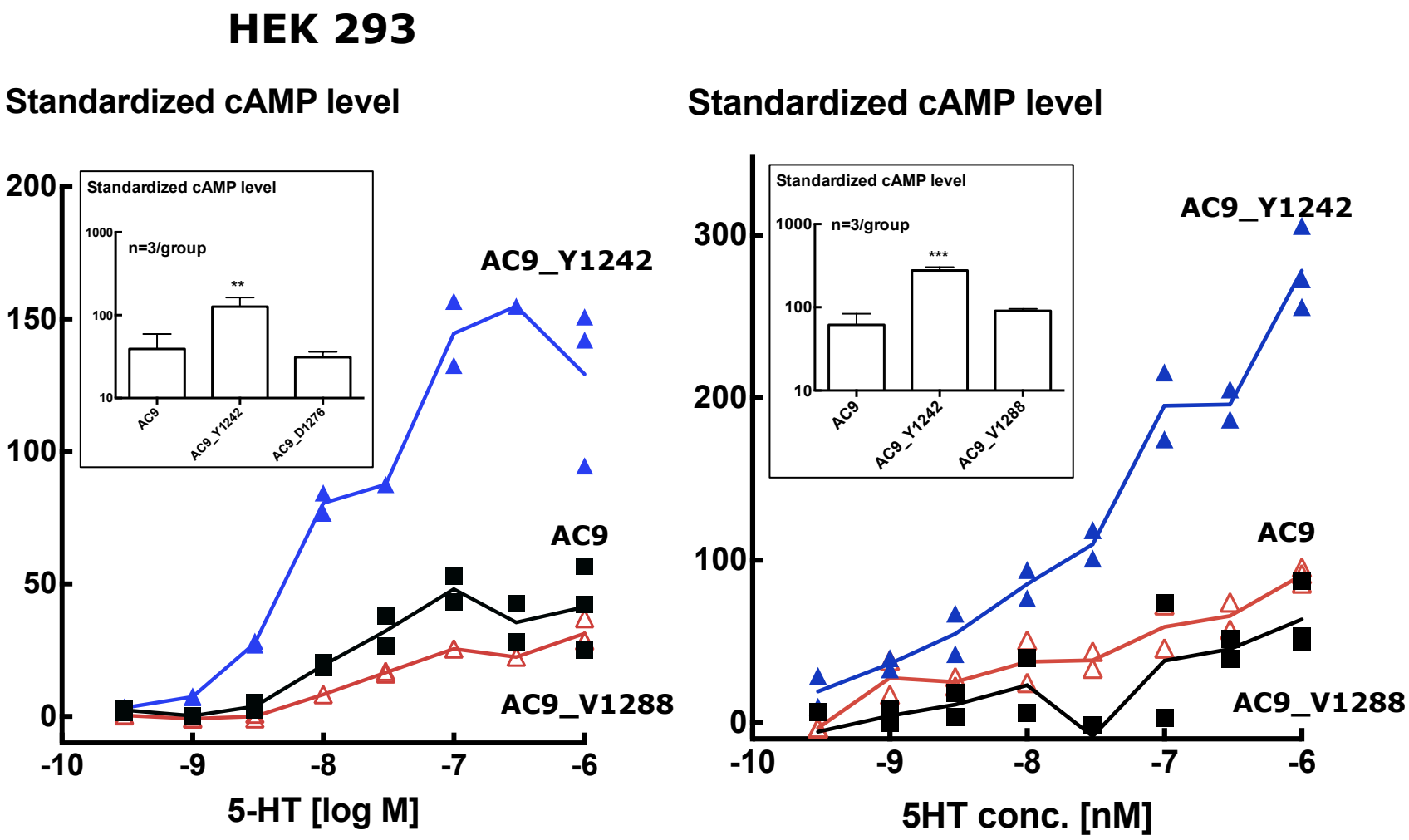
HEK 293
Standardized cAMP level
Standardized cAMP level
n=3/group
**
AC9
AC9_Y1242
AC9_D1276
AC9_Y1242
AC9
AC9_V1288
200
150
100
50
0
-10
-9
-8
-7
-6
5-HT [log M]
Standardized cAMP level
n=3/group
***
AC9
AC9_Y1242
AC9_V1288
AC9_Y1242
AC9
AC9_V1288
300
200
100
0
-10
-9
-8
-7
-6
5HT conc. [nM]

Fig. 5

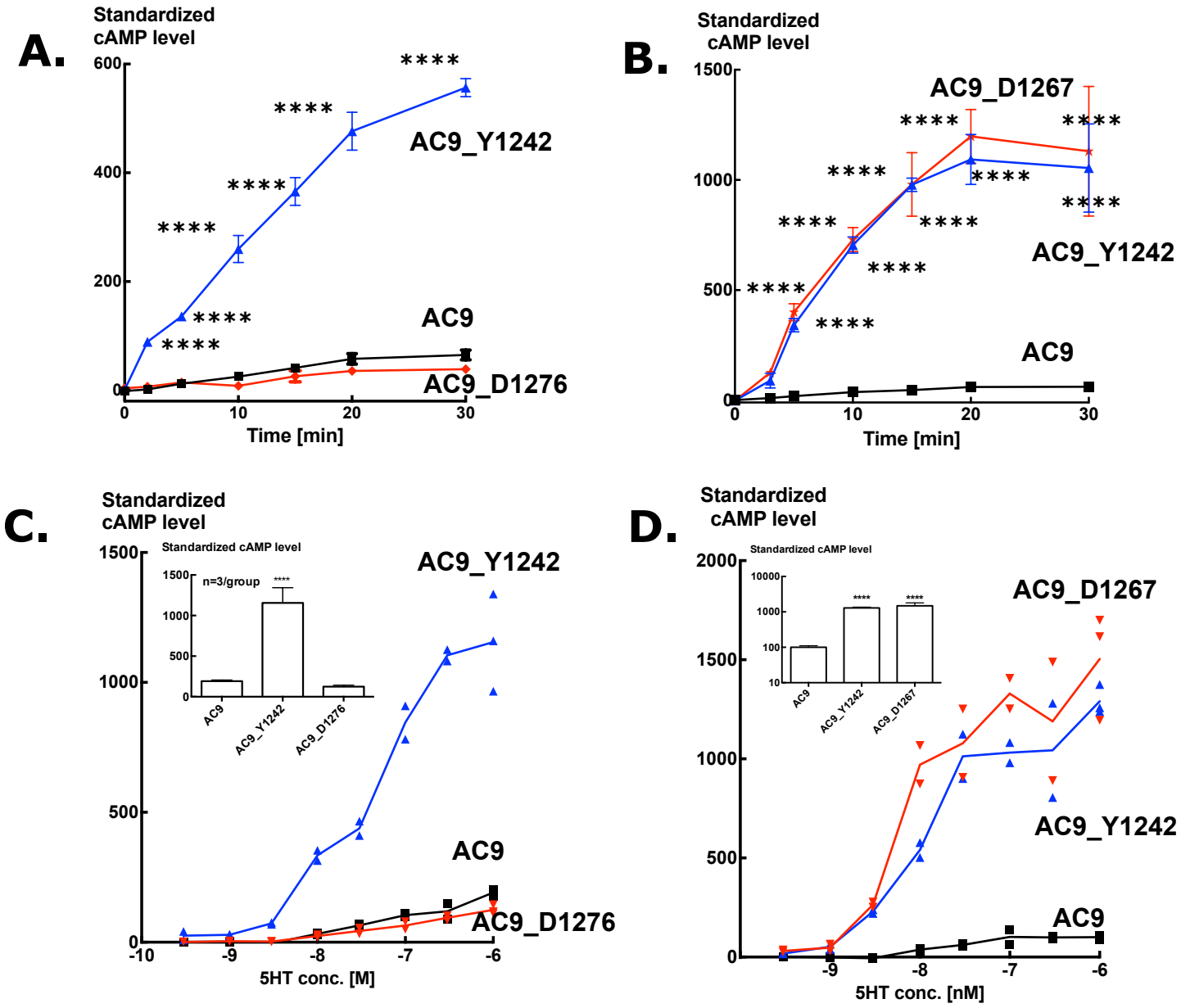
A.
Standardized cAMP level
600
400
200
0
0
10
20
30
Time [min]
****
AC9_Y1242
AC9
AC9_D1276
B.
Standardized cAMP level
1500
1000
500
0
AC9_D1267
AC9_Y1242
AC9
Time [min]
C.
Standardized cAMP level
1500
1000
500
0
-10
-9
-8
-7
-6
5HT conc. [M]
Standardized cAMP level
n=3/group
AC9
AC9_Y1242
AC9_D1276
AC9_Y1242
AC9
AC9_D1276
D.
Standardized cAMP level
2000
1500
1000
500
0
-9
-8
-7
-6
5HT conc. [nM]
Standardized cAMP level
10000
1000
100
10
AC9
AC9_Y1242
AC9_D1267
AC9_D1267
AC9_Y1242
AC9

Fig. 6

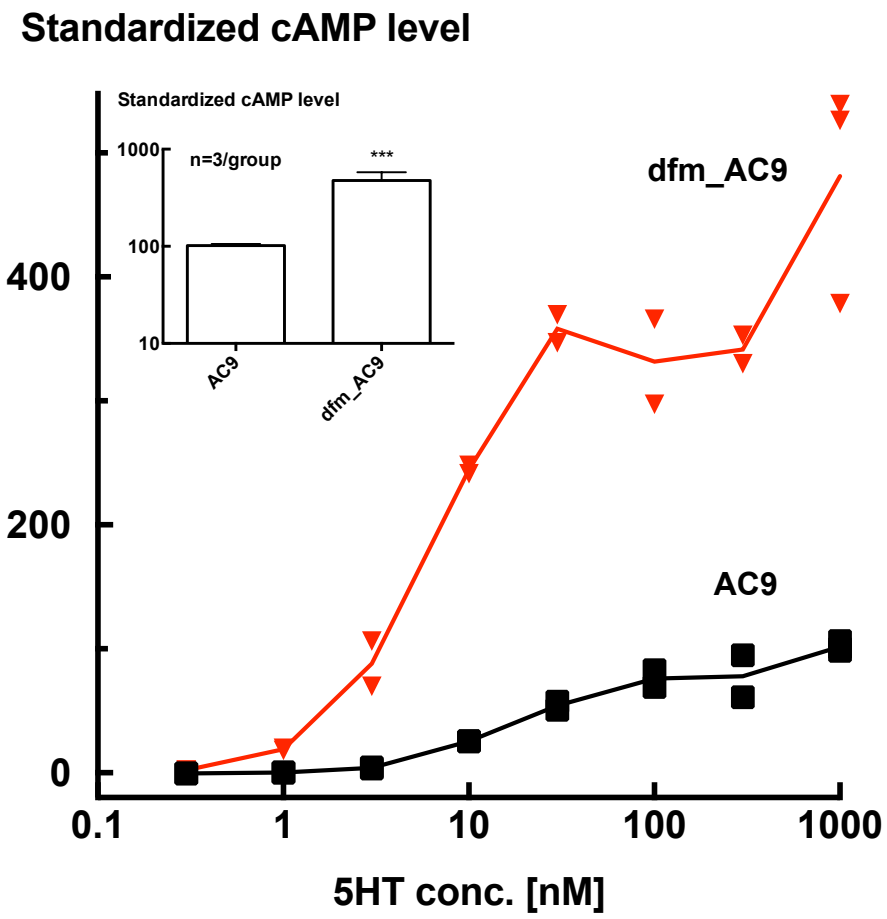
Standardized cAMP level
Standardized cAMP level
n=3/group
***
1000
100
10
AC9
dfm_AC9
dfm_AC9
AC9
400
200
0
0.1
1
10
100
1000
5HT conc. [nM]

Fig. 7

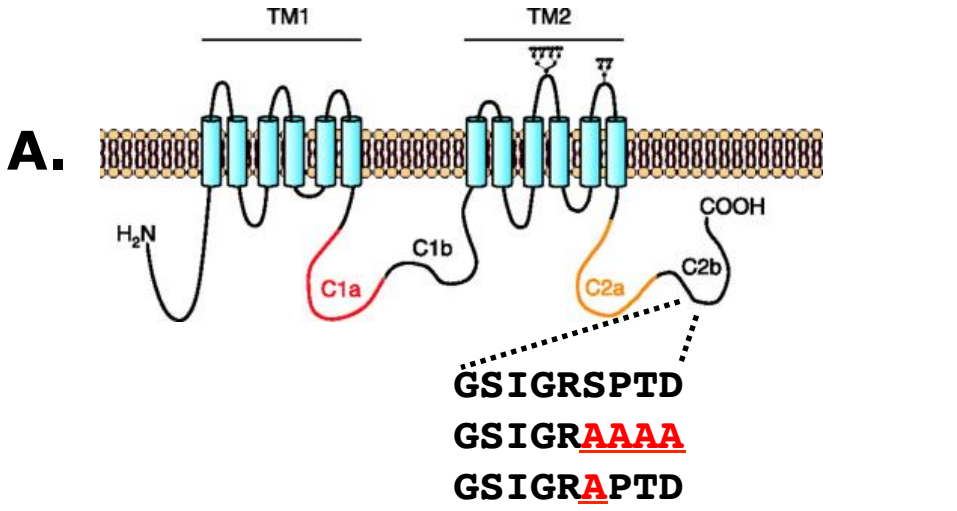
A.
TM1
TM2
H2N
C1a
C1b
C2a
C2b
COOH
GSIGRSPTD
GSIGRAAAA
GSIGRAPTD

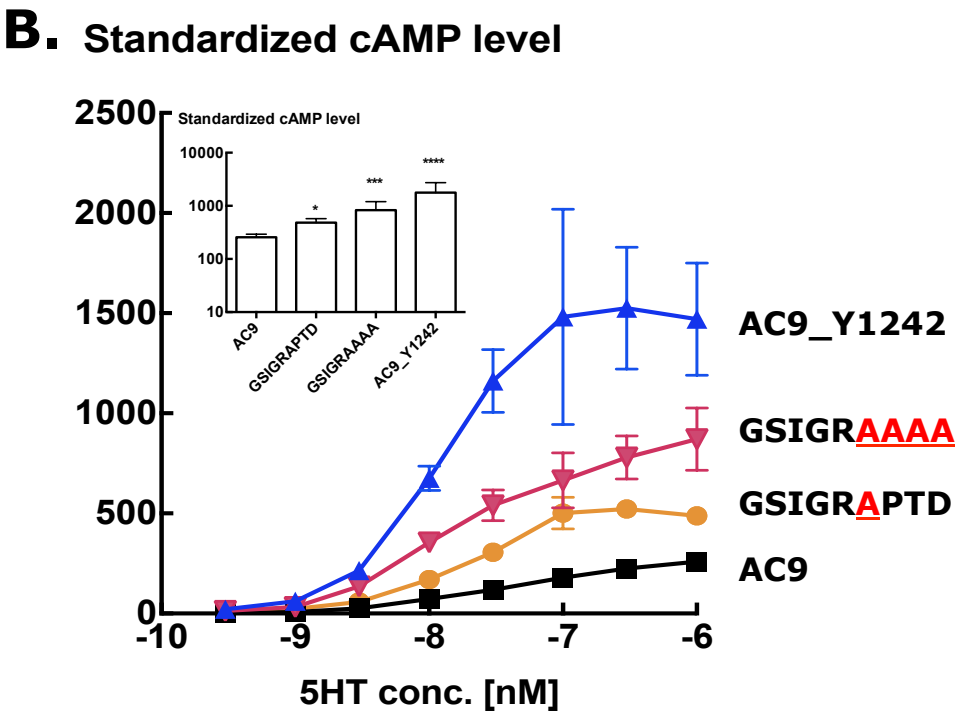
B. Standardized cAMP level
Standardized cAMP level
10000
1000
100
10
*
***
****
AC9
GSIGRAPTD
GSIGRAAAA
AC9_Y1242
2500
2000
1500
1000
500
0
-10
-9
-8
-7
-6
5HT conc. [nM]
AC9_Y1242
GSIGRAAAA
GSIGRAPTD
AC9

Fig. 8

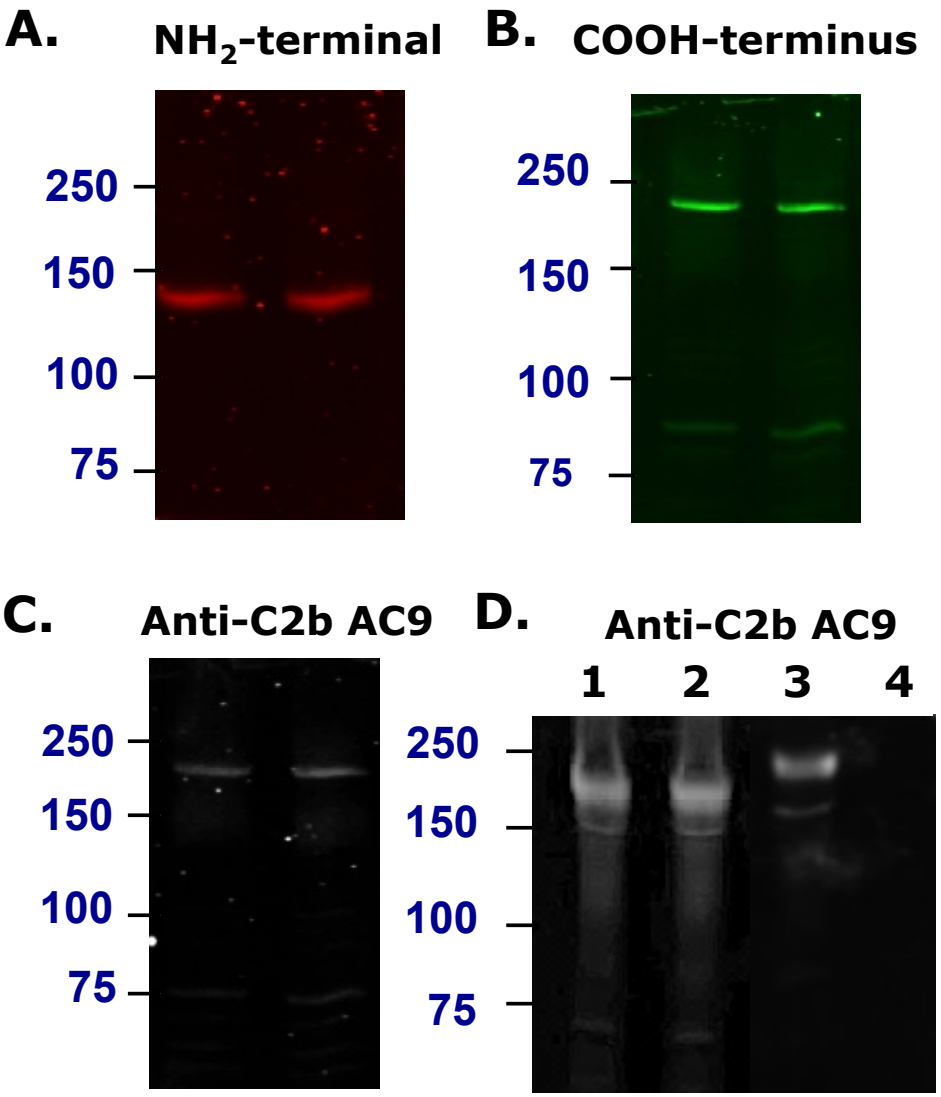
A.
NH2-terminal
250
150
100
75
B.
COOH-terminus
250
150
100
75
C.
Anti-C2b AC9
250
150
100
75
D.
Anti-C2b AC9
1
2
3
4
250
150
100
75

Fig. 9

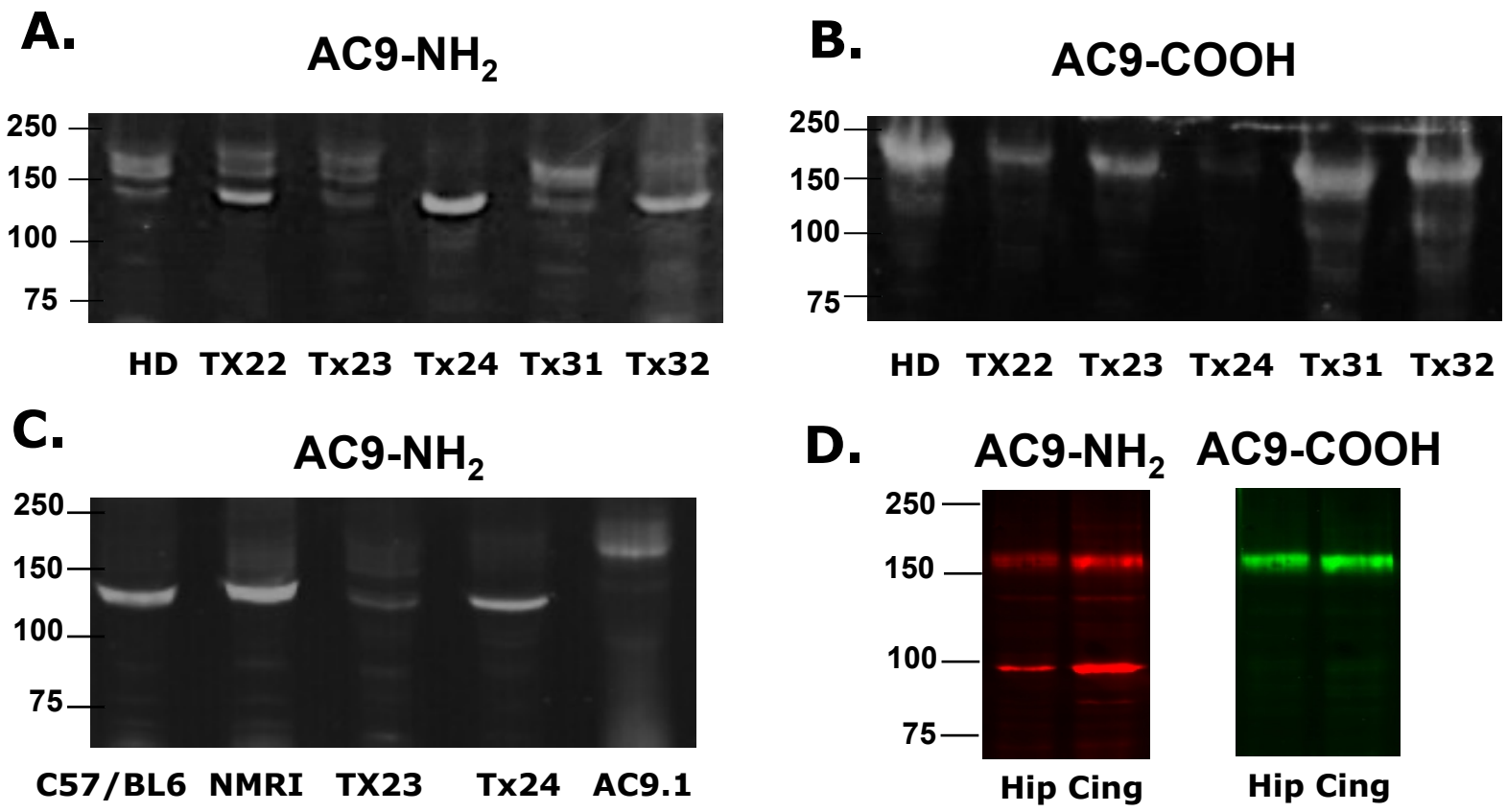
A.
AC9-NH2
250
150
100
75
HD TX22 Tx23 Tx24 Tx31 Tx32
B.
AC9-COOH
250
150
100
75
HD TX22 Tx23 Tx24 Tx31 Tx32
C.
AC9-NH2
250
150
100
75
C57/BL6 NMRI TX23 Tx24 AC9.1
D.
AC9-NH2
AC9-COOH
250
150
100
75
Hip Cing
Hip Cing

SUPPLEMENTARY DATA

Auto-inhibition of adenylyl cyclase 9 (AC9) by an isoform-specific motif in the carboxyl-terminal region. Pálvölgyi et al., Cellular Signalling.

1.0 Examination of the C2b domain sequence of mouse AC9 mRNA derived from different tissues

There are two reference sequences of *m. musculus* AC9 mRNA that were derived from genomic mapping of the mouse genome. Variant 1: Accession no. NM_009624 and Variant 2 Accession no. NM_001291910.

With respect to the latter "...variant (2) differs in the 5' UTR, lacks a portion of the 5' coding region, and initiates translation initiation at a downstream start codon, compared to variant 1. The encoded protein (isoform 2), has a shorter N-terminus than isoform 1."

Variant 1 is predicted to be comprised of 11, variant 2 from 12 exons. Significantly, the respective last exons in the two variants are identical and encode the COOH-terminal of the protein from the end of TM2 through C2a to C2b (see Fig. 1A of main article for nomenclature), from residue 957 to 1353. No potential mRNA splicing sites are apparent in the gene sequence. Similar considerations apply to the human AC9 gene (ADCY9, NG_011434.1).

Total RNA was prepared from frozen adult mouse (C57Bl/6J) hippocampus, brain cortex, and heart tissue by extraction with TRIzol/chloroform (Invitrogen) as per the manufacturers instructions. The isolation was continued by Qiagen RNeasy Kit with DNaseI treatment of samples (On Column DNase I Digestion Set, Sigma). The quality of the RNA preparation was assessed by gel electrophoresis on an Agilent Bioanalyzer 2100. The synthesis of cDNA was performed with Revert Aid First Strand cDNA Synthesis Kit (Fermentas) according to the manufacturer's description using 100 ng of each total RNA samples and oligo dT primers. Thereafter specific oligonucleotides were used to amplify by PCR the coding region of exon 11 of mouse AC9 (forward1, forward2, reverse1, see Supplementary Fig 1).

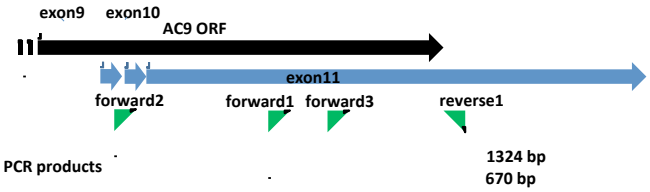

Table1. Mouse AC9 specific PCR primers (on the basis of NM_009624)

forward1	GGTTCAACTTCAAGCTCAGGGTCGGCT	exon11 (4239-4265 bp)
forward2	GTCAGGACAGTTCCATTGTGATG	exon9-10 (3585-3607 bp)
forward3	GTTATGACTTTGACTACCGAGGG	exon11 (4425-4447 bp) used for direct PCR product sequencing
reverse1	CTAGATAGCACAACAGCCTATCGAC	exon11 after stop codon (4908-4884 bp)

Supplementary Figure 1. Schematic summary of the analysis of mouse tissue AC9 mRNA by RT-PCR.

The PCR reaction was performed with Phusion High Fidelity DNA polymerase (Thermo Scientific) and was run as follows: 95 ºC for 5 min, followed by 33 cycles (95 ºC for 1 min, 62 ºC for 40 sec and 72 ºC for 25/45 sec) and a final extension step (72 ºC for 3 min). The PCR products (forward1-reverse: 670 bp, forward2-reverse: 1324 bp, see Supplementary Figs.1 and 2) were purified with the QIAquick PCR Purification Kit according to the protocol and verified by agarose gel electrophoresis. The DNA sequence was determined directly from the two PCR products in each sample with the gene-specific forward 3 and the reverse1 primer (Suppl. Fig 1). In addition, both PCR products obtained from heart tissue were subcloned into the pJET1.2 plasmid (Thermo Scientific) and the sequence of the amplified cDNA products (3-3 clones of each type) were determined using the standard pJET reverse and forward sequencing primers. The sequencing data of each sample were analyzed by assembling with the mRNA reference sequence (NM_009624) using Geneious software. DNA sequencing was carried out at Biomi Ltd, Gödöllő, Hungary.

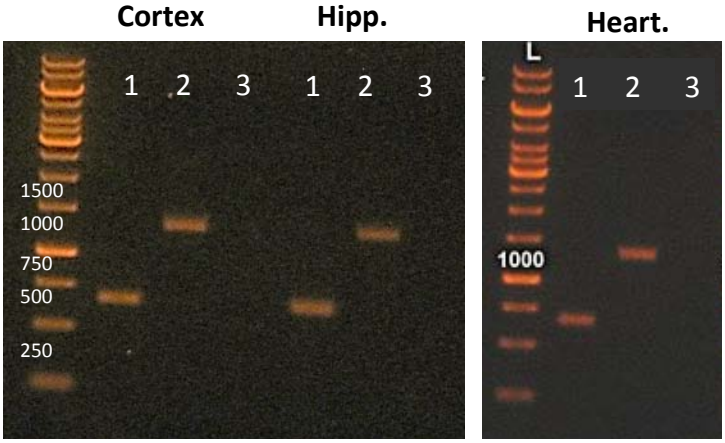

Supplementary Figure 2. RT-PCR for AC9 mRNA in mouse cerebral cortex, hippocampus (Hippo) and the left ventricle of the heart. Lane 1 : Primer Forward 1 and Reverse 1, Lane 2 : Primer Forward 2 and Reverse 1 Lane 3: Control for contaminating DNA in the RNA sample. Note expected products of 670 and 1324 bp in all three tissues.

The sequences of the two PCR products (Supplementary Fig. 2) were indetical to the reference mRNA sequence by direct sequencing and also after subcloning. One of the clones of the short PCR product had a single nucletide change from G to A at nucleotide (bp. 4337), which would result in a valine to isoleucine change at position 1191 at the protein level. Whether or not this is the result of DNA editing remains to be determined. However, it would not impact the immunoreaction with the either of the Anti-AC9 COOH-terminal antibodies used in this study.

There is a single gene for AC9 in both the mouse and the human genomes. Moreover, the exon_intron architecture of the mouse as well as the human AC9 genes is similar, in that residues 957-1353 (i.e. from the end of the TM2 domain through to the COOH-terminus) are encoded by a single, large exon. There are no apparent alternative mRNA splicing sites in this segment of either the mouse or the human gene. In agreement, we found no evidence for alternative C-terminal transcript variants of mouse AC9 that could explain the

presence of a COOH-terminally truncated AC9 protein in heart tissue. These findings are consonant with the computerized predictions derived from the sequence of exon 11 of the mouse gene as detailed at https://www.ncbi.nlm.nih.gov/nuccore/NM_009624.

With respect to exon 11, the same considerations apply to the human ADCY9 gene as to the mouse - https://www.ncbi.nlm.nih.gov/nuccore/NM_001116.3.

2.0 Verification of anti-AC9 antibodies in HEK293 cells expressing the skeleton vector pcDNA3.1.

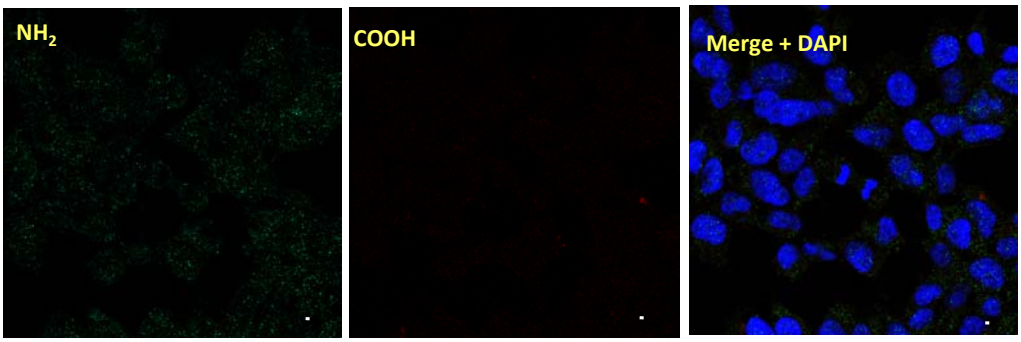

Supplementary Fig. 3. HEK293 cells stably expressing pcDNA3.1 were processed for immunostaining as detailed in section 2.5 of the article. Note the lack of meaningful reaction with either affinity-purified rabbit anti-AC9_NH_2-terminal region (NH_2, green) or affinity-purified anti-AC9_COOH-terminus (COOH, red) antibodies. The Merge panel includes the blue channel images resulting from staining with DAPI to reveal the cell nuclei. The bars represent 20μm. In contrast, the same antibodies produced intense labeling of HEK239 cells stably expressing human AC9 or AC9_Y1242. (see Fig. 2 of main paper). The anti-C2b rabbit serum received from R. Premont also failed to stain HEK293 cells expressing the skeleton vector (not shown).

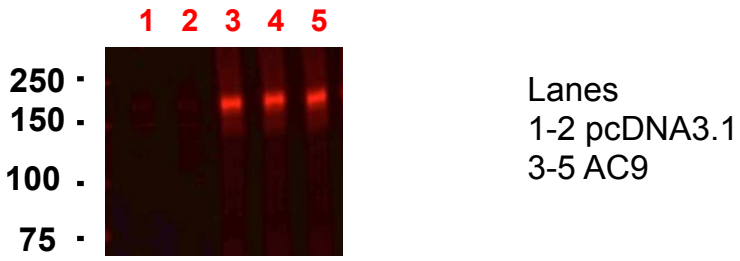

Supplementary Fig. 4. Immunoblots of crude membranes prepared from HEK293 cells stably expressing 5-HT_{7A} receptors and transfected with pcDNA3.1 or human AC9 reacted with affinity-purified rabbit anti-AC9 NH_2-terminal region antibodies. Note the absence of AC9 immunostaining in cells transfected the skeleton vector pcDNA3.1.

3.0 Raw cAMP data corresponding to Fig 4.and Fig 5. of the main paper.

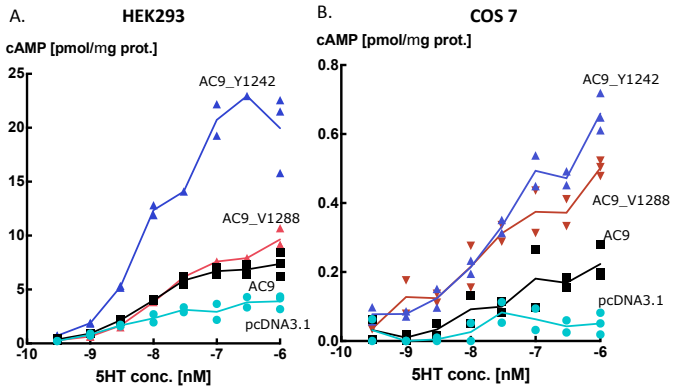

Supplementary Fig. 5 (corresponding to Fig. 4 of main paper)

A) HEK293 cells stably expressing 5-HT_{7A} receptors were transfected with pcDNA3.1, AC9, AC9_Y1242, AC9_V1288. The protocol for cAMP production in the presence of IBMX is described in section 2.3. B) COS-7 cells were co-transfected with the human 5-HT_{7A} receptor and pcDNA3.1, AC9, AC9_Y1242 or AC9_V1288. cAMP production in response to 5-HT was assessed as for HEK293 cells. Individual data points are shown.

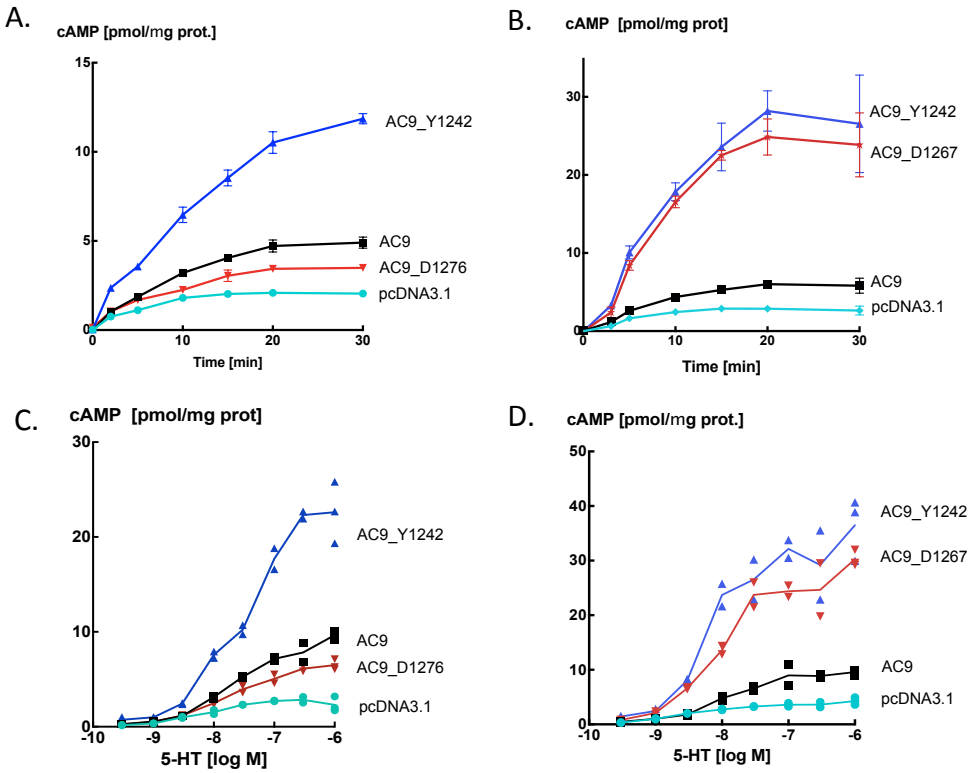

Supplementary Fig. 6 (corresponding to Fig. 5 of the main paper)

A &B) Time-course of cAMP production evoked by 15 nM 5-HT. Data are means±S.D. **C&D)** cAMP responses evoked by 5-HT, at 15 min after addition of the agonist. Note all-or-none type effect of the deletion of residues 1268-1277 on the 5-HT-induced cAMP response. Individual data points are shown.

4.0 The auto-inhibitory motif is in a phylogenetically highly conserved segment of the C2b domain.

```
XM_006897431.1              Elephantulus edwardii (Cape elephant shrew)
XM_022752346.1              Seriola dumerili (greater amberjack)
BC136658.1                  homo sapiens
Z50190.1                    mus musculus
XM_005306178.3              Chrysemys picta belli (Western painted turtle)
XM_009513803.1              Phalacrocorax carbo  (cormorant)
XM_010578353.1              Haliaeetus leucocephalus (bald eagle)


XM_006897431.1      MKTYLYPKCTDSGLVPQHQLSISPDIRVQVDGSIGRSPTDEIANLVPSVQTSDS------          54
XM_022752346.1      MKTYLYPKCTDNGVVPQHQLSISPDIRVQVDGSIGRSPTDEIANLVPSAQNADKTSLGSE          60
BC136658.1          MKTYLYPKCTDHRVIPQHQLSISPDIRVQVDGSIGRSPTDEIANLVPSVQYVDKTSLGSD          60
Z50190.1            MKTYLYPKCTDNGVVPQHQLSISPDIRVQVDGSIGRSPTDEIANLVPSVQYSDKASLGSD          60
XM_005306178.3      MKTYLYPKCMDNGVVPHHQLSISPDIRVQVDGSIGRSPTDEIANLVPSVQNSDKTSQGSD          60
XM_009513803.1      MKTYLYPKCMDNGIVPHHQLSISPDIRVQVDGSIGRSPTDEIANLVPSVQNSDKIAHGTD          60
XM_010578353.1      MKTYLYPKCMDNGIVPHHQLSISPDIRVQVDGSIGRSPTDEIANLVPSVQNSDKIAHGTD          60
                    ********* *  ::*:*****************************.*  *.

XM_006897431.1      -SPQARDAYASSQRPRREPVRAEERPLFSKAIERSDGEDTGLEDTNELTKLNTTKAM---          110
XM_022752346.1      NNAQAKDTHVSSKRLWKEPVKAEERCRFGKAIEKSDCEEMGMEEANELTKLNVSKSMPSA…        120
BC136658.1          SSTQAKDAHLSPKRPWKEPVKAEERGRFGKAIEKDDCDETGIEEANELTKLNVSKSV---          117
Z50190.1            DSTQAKEAHLSSKRSWREPVKAEERFPFGKAIEKDSCEDIGVEEASELSKLNVSKSV---          117
XM_005306178.3      NNLEPKDMLPSYKKLQKESLKAEDRCRFGKAV-KNDCEEAETEEVNELTKLNISKSV---          116
XM_009513803.1      N-SETRDIHPSTKKLQKDAVQAEERCRFGKATEKTGCEEAGTEEVNELTKLNISKSV---          116
XM_010578353.1      N-SETKDILPSAKKLQKDAVKAEERCRFGKAAEKTDCEEMGTEEVNELTKLNISKSV---          116
                       : ::   * ::  :: ::**:*  *.**  : . ::   *:..**:*** :*::
```

Supplementary Figure 7 Alignments of the C2b domain of AC9 of selected vertebrate species. Sequences that spanned most of the human AC9 COOH-terminal domain were selected. AC9 from further experimentally notable species such as zebrafish (*Danio rerio*) and *Xenopus laevis,* but for which the available sequences are much shorter, also show 100% conservation of the auto-inhibitory motif. Alignments were generated by the Clustal Omega server of the European Bioinformatics Institute, Hinxton, Cambridge, U.K.